Estimating illuminant direction and degree of surface relief

David C. Knill

Brown University, Department of Psychology, Providence, Rhode Island 02912

Received November 7, 1988; accepted September 6, 1989

Many algorithms for deriving surface shape from shading require an estimate of the direction of illumination. This paper presents a new estimator for illuminant direction, which also generates an estimate of the degree of surface relief, that is measured by the variance of surface orientation (the partial derivatives of surface depth). Surfaces are considered to be samples of a stochastic process representing depth as a function of position in the image plane. We derive an estimator for illuminant tilt that is based only on some general assumptions about the process. The assumptions are that the process is wide-sense stationary, strictly isotropic, and mean-square differentiable and that the second partial derivatives of surface depth are locally independent of the first partial derivatives. We develop an estimator of illuminant slant and degree of surface relief in two stages. In the first, we develop a general format for an estimator based on the same assumptions that are used for the tilt estimator. The second stage is the actual implementation of the estimator and requires the specification of a functional form for the local probability distribution of surface orientations. This approach contrasts with previous ones, which begin their development with an assumption of a particular distribution for surfaces. The approach has the advantage that it separates the problems of surface modeling and light-source estimation, permiting one to easily implement specific estimators for different surface models. We implement the illuminant slant estimator for surfaces that have a Gaussian distribution of surface orientations and show simulation results. Degraded performance in the presence of self-shadowing is discussed.

1. INTRODUCTION

A primary goal of any visual system, biological or artificial, is to extract information about the three-dimensional structure of the environment from a dynamic two-dimensional image. This problem is one of inverse optics, in which the goal is to invert the imaging function that maps a scene to one or more images. The images are functions of scene characteristics such as shape, reflectance, depth relations between objects, illuminant geometry (number, position, and types of illuminants), and camera parameters. In most cases, information in the images that is useful for the derivation of one scene variable is coupled to other variables as well. A good example is the relationship between the estimation of illuminant direction and surface shape in the use of shading information. Most models that are used to determine shape from shading require knowledge of the illuminant direction.[1–3] The one model that does not[4] relies on a too strong assumption of surface geometry, namely that all surface points are umbilical (surface patches are locally spherical). Current models for estimating illuminant direction depend on the assumption of a particular probability distribution of surfaces. One would like, however, to have an estimator that could be easily modified to fit different distributions, which would effectively separate the problems of surface modeling and light-source estimation. In this paper, we derive the general format of an estimator that can be implemented using any surface distribution that fits some basic criteria.

The light energy reflected to the viewer from a surface, with the simplifying assumption of a point light source and matte surfaces, is given by the Lambertian shading equation

$$I = \rho\lambda(\vec{N} \cdot \vec{L}), \tag{1}$$

where I is the luminance, ρ is the surface reflectance, λ is the light energy flux incident on the surface, $\vec{N}$ is the surface-normal vector at a point, and $\vec{L}$ is a unit vector in the direction of the light source.

In a coordinate system (x, y, z), where z is taken to be positive in the direction of the viewer, we can represent $\vec{N}$ as the vector $(n_x, n_y, n_z)^T$, whose components are given by

$$n_x = \frac{-p}{\sqrt{p^2 + q^2 + 1}}, \tag{2}$$

$$n_y = \frac{-q}{\sqrt{p^2 + q^2 + 1}}, \tag{3}$$

$$n_z = \frac{1}{\sqrt{p^2 + q^2 + 1}}, \tag{4}$$

where

$$p = \frac{\partial z}{\partial x}, \qquad q = \frac{\partial z}{\partial y}. \tag{5}$$

Note that $n_z \geq 0$, which will always be the case for surface points projected to the viewer. The illuminant vector $\vec{L}$ is written as $(l_x, l_y, l_z)^T$. Expanding Eq. (1) for the shading equation, we obtain

$$I = \rho\lambda(n_x l_x + n_y l_y + n_z l_z). \tag{6}$$

Figure 1 summarizes the imaging geometry.

We can also write Eq. (1) as

$$I = \rho\lambda \cos\beta, \tag{7}$$

where β is the angle between the surface normal and the illuminant direction. Using this formulation, we find it convenient to represent the surface normal and the illuminant vector by their slants and tilts. The slant of a vector is the angle made by the vector and the z axis. The tilt of a

0740-3232/90/040759-17$02.00

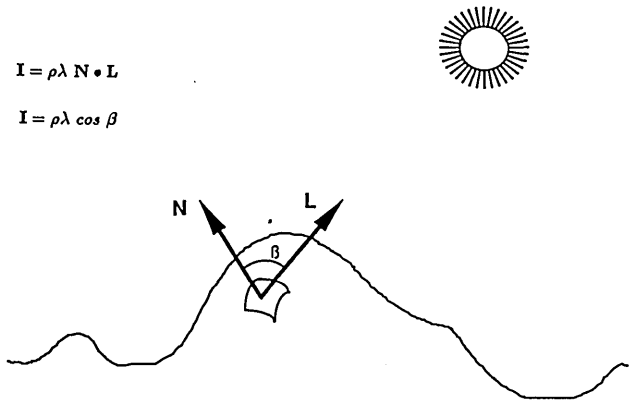

Fig. 1. Imaging geometry assumed for the discussion. All vectors are represented in a three-dimensional coordinate system, in which the z axis points toward the viewer. The x–y plane perpendicular to this direction is referred to as the image plane. Local surface orientation is represented by a normal vector $\vec{N}$. The unit vector $\vec{L}$ points toward the light source. For matte surfaces, the percentage of light energy reflected to the viewer from a point is given by the cosine of the angle β between $\vec{N}$ and $\vec{L}$. Orthographic projection of the surface to the image is assumed.

vector is its angle away from the horizontal in the image plane. Surface slant and tilt are related to the normal vector by

$$s = \cos^{-1}(n_z), \tag{8}$$

$$\tau = \tan^{-1}(n_y/n_x), \tag{9}$$

and similarly for the illuminant direction

$$s_l = \cos^{-1}(l_z), \tag{10}$$

$$\tau_l = \tan^{-1}(l_y/l_x). \tag{11}$$

The problem of estimating illuminant direction is to find the vector $\vec{L}$ from an image of a shaded surface or a collection of shaded surfaces. Knowledge of the shapes of surfaces in an image would greatly simplify the determination of illuminant direction. This information is not generally available, however, as knowledge of the illuminant direction is often necessary for the initial determination of surface shape. One may, however, use knowledge of the statistical structure of surfaces in the estimation of $\vec{L}$. If we model surfaces as being samples of a stochastic process, then the statistical structure of images of these surfaces will depend jointly on the structure of the surfaces and the illuminant direction. Using knowledge of the biasing effects of the illuminant on image statistics, we can derive a good estimate of the illuminant direction.

The estimators of Pentland[5] and Lee and Rosenfeld[2] rely on the assumption that the statistical structure of surfaces may be approximated by that of spheres. Both estimators make use of the means of partial derivatives of image luminance $\partial I/\partial r_\theta$ that are computed in different directions θ in the image. The simulations that were reported by the authors deal only with spheres, ellipsoids, and, in Pentland's case, images of some naturally occurring, simply convex objects. The assumption of convexity, however, seems to be overly restrictive for the surfaces that make up visual scenes. Many surfaces will extend beyond the boundaries of images and will be of mixed type, that is, will have both convex and concave regions, as well as hyperbolic, parabolic, and planar regions. Neither of the estimators will work for surfaces that are not predominantly convex. The distribution of $\partial\vec{N}/\partial r_\theta$ is symmetric around zero for such surfaces, so that $E[\partial\vec{N}/\partial r_\theta] = 0$. From Eq. (6), we see that this distribution implies that $E[\partial\mathbf{I}/\partial r_\theta] = 0$, so that neither tilt estimator would work, nor would Lee and Rosenfeld's slant estimator. Figure 2 demonstrates clearly that humans are able to estimate, at least coarsely, illuminant direction for images of surfaces that are drawn from an ensemble for which $E[\partial\vec{N}/\partial r_\theta] = 0$. Most people who look at this image have the correct impression of a light source coming from the upper-left-hand corner.

In the following sections, we derive an estimator for illuminant tilt and the general format of an estimator for illuminant slant that are based only on some reasonable assumptions about the ensemble of surfaces that make up visual scenes. Surfaces are considered to be samples of a two-dimensional stochastic process that specifies surface depth at points in the image plane. Derivation of the estimators requires four assumptions about the surface process:

1. The process is wide-sense stationary; that is, the correlation and mean functions of the process are invariant over position in the image plane.
2. The process is strictly isotropic; that is, the probability law of the process is invariant over rotations of the coordinate system in which it is defined (see definition in Appendix A).
3. The process is mean-square differentiable.[6]
4. The second-order partial derivatives at a point are independent of the first-order partial derivatives at that point; that is, the curvature of the surface is locally independent of the orientation.

The last assumption may not be as constraining as it first appears because the nth-order partial derivatives of a stationary process can be proven to be locally uncorrelated with

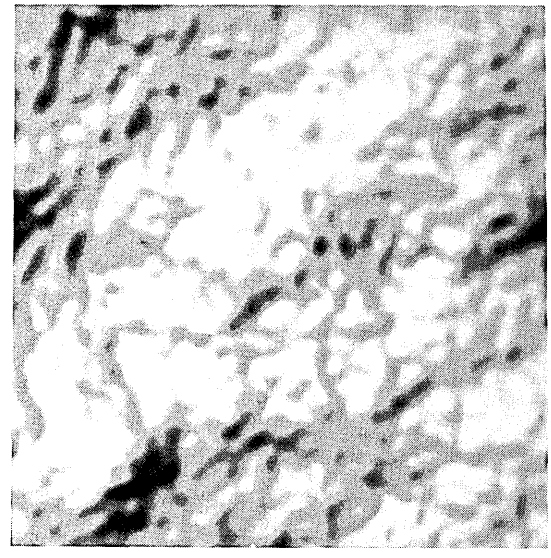

Fig. 2. Image of a smoothed fractal surface illuminated by a point light source at 135° tilt and 30° slant (from the upper-left-hand corner). The surface has a fractal dimension of 2.2 and has been smoothed by low-pass filtering of the depth values.

the lower-order derivatives (Proposition A1, Appendix A). They are therefore independent for Gaussian surface processes.

In order to avoid the necessity for a full specification of a model of surface statistics, we use only local moments of image luminance and its derivatives for the estimators. In particular, we use the mean and variance of image luminance and its derivatives computed in orthogonal directions. We show that a good estimate of illuminant tilt is given by the direction in which the variance of luminance change is greatest. The interaction between the illuminant slant and the structure of the surface process is more complex, and estimation of illuminant slant necessitates the simultaneous estimation of the degree of relief of surfaces, as measured by the variance of the partial derivatives of surface depth. Two statistics are needed, therefore, for the estimation of these two parameters. We use the average mean-square contrast of the image (luminance variance divided by the square of the mean luminance) and the ratio of the variances of luminance change in two directions, one parallel to the estimated illuminant tilt and one orthogonal to it. Actual implementation of the slant estimator requires only the selection of a functional form for the local probability distribution of surface orientation parameterized by its mean and variance (e.g., Gaussian versus exponential).

Section 2 gives definitions of the variables used in this paper. Sections 3 and 4 present derivations of the two estimators. The derivations make use of some of the local properties of the stochastic processes that could represent surfaces. Proofs of these properties are given in Appendixes A and B. Section 5 describes an implementation of the slant estimator for surfaces with a Gaussian distribution of orientations. Simulation results are given in Section 6. Propositions given in the appendixes are labeled according to the appendix in which they can be found; e.g., Proposition A2 is found in Appendix A.

2. DEFINITIONS

We define $\mathbf{S}(x, y)$ to be a stochastic process representing surface depth on a two-dimensional lattice. $\mathbf{S}(x, y)$ is a random function that is indexed by spatial position (x, y) and can be viewed as a set of random variables arranged on the lattice. Such a stochastic process may be characterized by the conditional probability densities that describe the dependence of $\mathbf{S}(x_1, y_1)$ on $\mathbf{S}(x_2, y_2)$, where (x_1, y_1) and (x_2, y_2) are different points on the lattice. Alternatively, the process may be characterized by its summary statistics, such as its mean and variance functions, which specify the mean and variance of $\mathbf{S}(x, y)$ at each point on the lattice. Since we have assumed that $\mathbf{S}(x, y)$ is wide-sense stationary, these functions are constants that do not vary with spatial position. Since we consider only the class of wide-sense stationary stochastic processes here, we will drop the index in our notation, to indicate that the derived expectations are independent of spatial position.

$\mathbf{S}$ is the model for those regions of surfaces in the environment that are projected to an image under orthographic projection, with the lattice corresponding to the image plane. We define stochastic processes for the partial derivatives of $\mathbf{S}$ as

$$\mathbf{P} = \frac{\partial \mathbf{S}}{\partial x}, \tag{12}$$

$$\mathbf{Q} = \frac{\partial \mathbf{S}}{\partial y}, \tag{13}$$

$$\mathbf{P}_x = \frac{\partial \mathbf{P}}{\partial x} = \frac{\partial^2 \mathbf{S}}{\partial x^2}, \tag{14}$$

$$\mathbf{Q}_y = \frac{\partial \mathbf{Q}}{\partial y} = \frac{\partial^2 \mathbf{S}}{\partial y^2}, \tag{15}$$

$$\mathbf{P}_y = \frac{\partial \mathbf{P}}{\partial y} = \frac{\partial^2 \mathbf{S}}{\partial x \partial y} = \frac{\partial \mathbf{Q}}{\partial x} = \mathbf{Q}_x. \tag{16}$$

The surface-normal vectors are represented by a vector-valued stochastic process

$$\vec{\mathbf{N}} = (\mathbf{n}_x, \mathbf{n}_y, \mathbf{n}_z)^T, \tag{17}$$

where

$$\mathbf{n}_x = \frac{-\mathbf{P}}{\sqrt{\mathbf{P}^2 + \mathbf{Q}^2 + 1}}, \tag{18}$$

$$\mathbf{n}_y = \frac{-\mathbf{Q}}{\sqrt{\mathbf{P}^2 + \mathbf{Q}^2 + 1}}, \tag{19}$$

$$\mathbf{n}_z = \frac{1}{\sqrt{\mathbf{P}^2 + \mathbf{Q}^2 + 1}}. \tag{20}$$

Finally, we define processes for the local slant and tilt of surfaces:

$$\mathbf{\Sigma} = \cos^{-1}(\mathbf{n}_z) = \cos^{-1}\frac{1}{\sqrt{\mathbf{P}^2 + \mathbf{Q}^2 + 1}}, \tag{21}$$

$$\mathbf{T} = \tan^{-1}\left(\frac{\mathbf{n}_y}{\mathbf{n}_x}\right) = \tan^{-1}\left(\frac{\mathbf{Q}}{\mathbf{P}}\right). \tag{22}$$

3. ESTIMATING ILLUMINANT TILT

The means of luminance change in an image are, in general, inappropriate for the estimation of illuminant tilt, as discussed in Section 1. The logical alternative is to use higher-order moment functions (e.g., variance of luminance change) for the estimation. Looking at Fig. 2, you may note that luminance seems to change more sharply along the diagonal that runs from the upper-left-hand corner of the image to the lower-right-hand corner. This direction does, in fact, correspond to the tilt of the illuminant used in generating the image. The observation leads to the tilt estimator, as stated formally in Proposition 1.

Proposition 1

Let $\mathbf{S}$ be a wide-sense stationary, strictly isotropic, mean-square differentiable, two-dimensional stochastic process that represents surface depths in the image plane. Furthermore, let the second-order partial derivatives of $\mathbf{S}$ be locally independent of the first-order partial derivatives. Let $\mathbf{I}$ represent the image onto which light reflected from $\mathbf{S}$ is projected under orthographic projection. $\partial \mathbf{I}/\partial r_\theta$ is the partial derivative of $\mathbf{I}$ that is computed in a direction θ in the image. If the surface represented by $\mathbf{S}$ has Lambertian reflectance and is illuminated by a point source at infinity, the tilt of the illuminant is given by the angle θ for which the

variance of $\partial \mathbf{I}/\partial r_\theta$ is greatest. This is the angle θ, which maximizes[7]

$$E\left[\left(\frac{\partial \mathbf{I}}{\partial r_\theta}\right)^2\right] = E\left[\left(\frac{\partial \mathbf{I}}{\partial x}\right)^2\right]\cos^2\theta + E\left[\left(\frac{\partial \mathbf{I}}{\partial y}\right)^2\right]\sin^2\theta + 2E\left[\left(\frac{\partial \mathbf{I}}{\partial x}\right)\left(\frac{\partial \mathbf{I}}{\partial y}\right)\right]\sin\theta\cos\theta, \quad (23)$$

and is given by

$$\hat{\tau}_l = \hat{\theta} = \frac{1}{2}\tan^{-1}\frac{2E[(\partial \mathbf{I}/\partial x)(\partial \mathbf{I}/\partial y)]}{E[(\partial \mathbf{I}/\partial x)^2] - E[(\partial \mathbf{I}/\partial y)^2]}. \quad (24)$$

Proof

For convenience, we will use a coordinate system that is aligned with the illuminant tilt for the proof. In this coordinate system, the illuminant vector is given by

$$\vec{L} = (l_x, 0, l_z)^T. \quad (25)$$

It is necessary to show that $E[(\partial \mathbf{I}/\partial r_\theta)^2]$ is greatest for $\theta = 0$ in this coordinate system. $\mathbf{I}$ is given by

$$\mathbf{I} = \rho\lambda(\mathbf{n}_x l_x + \mathbf{n}_z l_z), \quad (26)$$

and the partial derivative, computed along a direction θ, is given by

$$\frac{\partial \mathbf{I}}{\partial r_\theta} = \rho\lambda\left[\left(\frac{\partial \mathbf{n}_x}{\partial r_\theta}\right)l_x + \left(\frac{\partial \mathbf{n}_z}{\partial r_\theta}\right)l_z\right]. \quad (27)$$

The function that we want to maximize is the variance

$$E\left[\left(\frac{\partial \mathbf{I}}{\partial r_\theta}\right)^2\right] = \rho^2\lambda^2 E\left[\left(\frac{\partial \mathbf{n}_x}{\partial r_\theta}l_x + \frac{\partial \mathbf{n}_z}{\partial r_\theta}l_z\right)^2\right]. \quad (28)$$

The cross term $E[(\partial \mathbf{n}_x/\partial r_\theta)(\partial \mathbf{n}_z/\partial r_\theta)]$ goes to zero (Proposition A6), so we have

$$E\left[\left(\frac{\partial \mathbf{I}}{\partial r_\theta}\right)^2\right] = \rho^2\lambda^2\left\{l_x^2 E\left[\left(\frac{\partial \mathbf{n}_x}{\partial r_\theta}\right)^2\right] + l_z^2 E\left[\left(\frac{\partial \mathbf{n}_z}{\partial r_\theta}\right)^2\right]\right\}. \quad (29)$$

For isotropic surfaces, $\mathbf{n}_z$ is independent of the orientation of the coordinate system (Proposition A4), so the second term is constant for all θ's, and we need only maximize the function

$$f(\theta) = \rho^2\lambda^2 l_x^2 E\left[\left(\frac{\partial \mathbf{n}_x}{\partial r_\theta}\right)^2\right]. \quad (30)$$

Writing this in terms of the partial derivatives $\partial \mathbf{n}_x/\partial x$ and $\partial \mathbf{n}_x/\partial y$, we get

$$f(\theta) = \rho^2\lambda^2 l_x^2 E\left[\left(\cos\theta\frac{\partial \mathbf{n}_x}{\partial x} + \sin\theta\frac{\partial \mathbf{n}_x}{\partial y}\right)^2\right]. \quad (31)$$

The cross term $E[(\partial \mathbf{n}_x/\partial x)(\partial \mathbf{n}_x/\partial y)]$ goes to zero (Proposition A6), which leaves, with some simpification,

$$f(\theta) = \rho^2\lambda^2 l_x^2\left\{\cos^2\theta E\left[\left(\frac{\partial \mathbf{n}_x}{\partial x}\right)^2\right] + \sin^2\theta E\left[\left(\frac{\partial \mathbf{n}_x}{\partial y}\right)^2\right]\right\}. \quad (32)$$

Taking the derivative and setting it equal to zero, we get the relation

$$\sin\theta\cos\theta E\left[\left(\frac{\partial \mathbf{n}_x}{\partial x}\right)^2\right] = \sin\theta\cos\theta E\left[\left(\frac{\partial \mathbf{n}_x}{\partial y}\right)^2\right]. \quad (33)$$

This has the solutions $\theta = 0$, $\theta = \pi/2$ for cases in which $E[(\partial \mathbf{n}_x/\partial x)^2] \neq E[(\partial \mathbf{n}_x/\partial y)^2]$. Substituting back into Eq. (32) for $f(\theta)$, we have for $\theta = 0$

$$f(0) = \rho^2\lambda^2 l_x^2 E\left[\left(\frac{\partial \mathbf{n}_x}{\partial x}\right)^2\right], \quad (34)$$

and for $\theta = \pi/2$

$$f(\pi/2) = \rho^2\lambda^2 l_x^2 E\left[\left(\frac{\partial \mathbf{n}_x}{\partial y}\right)^2\right]. \quad (35)$$

Except for the degenerate case of a planar surface, one can easily show that $E[(\partial \mathbf{n}_x/\partial x)^2] > E[(\partial \mathbf{n}_x/\partial y)^2]$ [Appendix B, Eqs. (B7) and (B8)]. $\theta = 0$ is, therefore, a maximum of the function, while $\theta = \pi/2$ is a minimum of the function. As one would expect, the derivative computed along a direction orthogonal to the tilt of the illuminant has the minimal variance.

The function to be maximized in estimating the tilt is

$$E\left[\left(\frac{\partial \mathbf{I}}{\partial r_\theta}\right)^2\right] = E\left[\left(\frac{\partial \mathbf{I}}{\partial x}\cos\theta + \frac{\partial \mathbf{I}}{\partial y}\sin\theta\right)^2\right],$$

$$E\left[\left(\frac{\partial \mathbf{I}}{\partial r_\theta}\right)^2\right] = E\left[\left(\frac{\partial \mathbf{I}}{\partial x}\right)^2\right]\cos^2\theta + E\left[\left(\frac{\partial \mathbf{I}}{\partial y}\right)^2\right]\sin^2\theta + 2E\left[\left(\frac{\partial \mathbf{I}}{\partial x}\right)\left(\frac{\partial \mathbf{I}}{\partial y}\right)\right]\sin\theta\cos\theta. \quad (36)$$

Taking the derivative of Eqs. (36) with respect to θ and setting it equal to zero, we obtain

$$\frac{\sin\hat{\theta}\cos\hat{\theta}}{\cos^2\hat{\theta} - \sin^2\hat{\theta}} = \frac{E[(\partial \mathbf{I}/\partial x)(\partial \mathbf{I}/\partial y)]}{E[(\partial \mathbf{I}/\partial x)^2] - E[(\partial \mathbf{I}/\partial y)^2]},$$

$$\frac{1}{2}\tan 2\hat{\theta} = \frac{E[(\partial \mathbf{I}/\partial x)(\partial \mathbf{I}/\partial y)]}{E[(\partial \mathbf{I}/\partial x)^2] - E[(\partial \mathbf{I}/\partial y)^2]},$$

$$\hat{\theta} = \frac{1}{2}\tan^{-1}\frac{2E[(\partial \mathbf{I}/\partial x)(\partial \mathbf{I}/\partial y)]}{E[(\partial \mathbf{I}/\partial x)^2] - E[(\partial \mathbf{I}/\partial y)^2]}. \quad (37)$$

Q.E.D.

The illuminant tilt is given by the solution to Eqs. (37), which maximizes Eqs. (36).

4. ESTIMATING ILLUMINANT SLANT AND DEGREE OF RELIEF

Estimation of the illuminant slant poses a more severe problem than the estimation of the tilt because the illuminant slant is confounded with the statistical properties of surfaces in all local image statistics. Luminance contrast is a good example of this problem because it increases with increases in illuminant slant or with increases in the degree of relief of surfaces. Figure 3 shows two images that have approximately equal luminance contrast, despite being generated with light sources at different slants. The illuminant slant is greater in one image, but the degree of relief in the other is greater (which makes the hills and valleys more peaked). The differences in illuminant slant and degree of relief conspire to keep the contrast between the images equal. Because of the confound between the illuminant slant and the statistical properties of the surface, the best that we can do is to use image statistics that can be expressed as functions of only one parameter of the surface process. This will leave

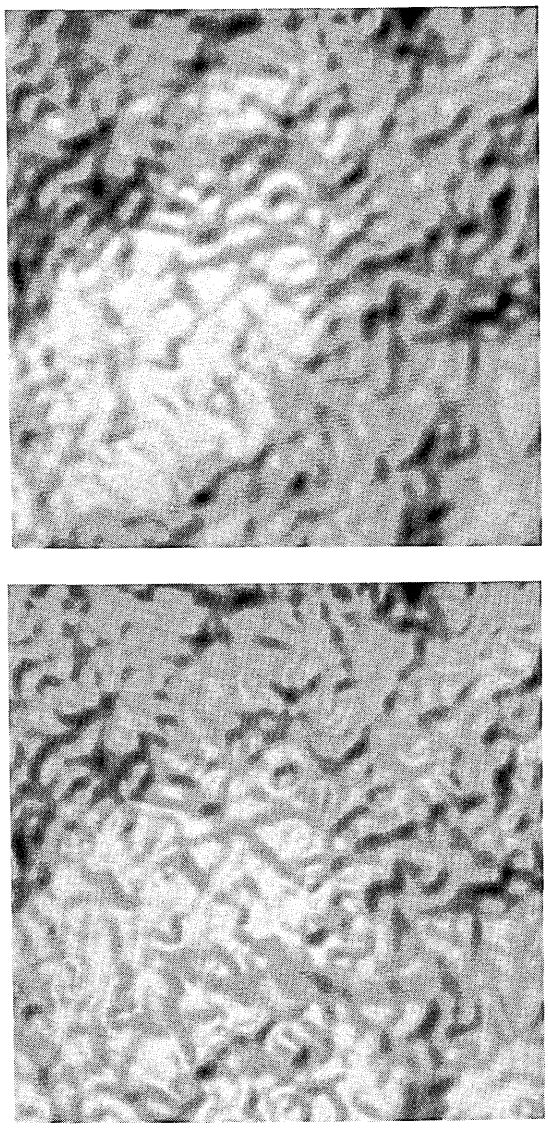

Fig. 3. a, Smoothed fractal surface illuminated by a point light source at 135° tilt and 30° slant. b, This image shows the same surface after being stretched along the viewing direction (z axis) (the depths were scaled by a factor of 2) and illuminated by a source at a shallower slant (15°). The differences in the degree of relief in the surfaces and in the slant of the illuminant conspire to keep the average contrasts in the two images approximately equal.

two unknowns that need to be solved for, the value of the parameter and the illuminant slant. The example above suggests using a parameter that corresponds to the degree of relief of surfaces in a scene. Looking at Fig. 3, see if you can tell in which picture the sun is higher in the sky and in which the degree of surface relief is greater. Most people are able to categorize the images correctly, suggesting that we are able to disentangle the effects of illuminant slant and surface relief on the image statistics.

Pentland uses a strategy similar to the one that was just described. He models surfaces as spheres and relates the mean and variance of luminance change in an image to the illuminant slant and the radius of the projected sphere. We would, however, like to avoid specifying an *a priori* model of surfaces in the development of an estimator.

In this section, we derive two image statistics that can be expressed as functions of the illuminant slant and the statistical moments of the z component of surface normals, $E[\mathbf{n}_z{}^i]$ ($i > 0$). The moments, $E[\mathbf{n}_z{}^i]$, can be related to the parameters that specify the local distribution of surface orientation, $f_{\mathbf{p}}(p)$. (The distributions of $\mathbf{P}$ and $\mathbf{Q}$ are equivalent for isotropic surface processes.) If the distribution is parameterized by its mean and variance, the statistics will reduce to functions of the illuminant slant and the variance of surface orientation, since the means of $\mathbf{P}$ and $\mathbf{Q}$ are known to be zero [Appendix A, Eq. (A2)]. The variance of $\mathbf{P}$ and $\mathbf{Q}$ provides a measure of the degree of relief in a surface. Note that only the form of the local distribution of $\mathbf{P}$ needs to be specified. It is not necessary to model the entire multivariate distribution of the surface process (no assumptions need be made, for example, about the correlational structure of surfaces).

The most obvious statistics to use are the mean and variance of image luminance. These parameters, however, depend on ρ and λ. Luminance contrast, on the other hand, does not. It is defined as the variation of image luminance around its mean, normalized by the square of the mean, and is given by

$$C = \frac{E[(\mathbf{I} - E[\mathbf{I}])^2]}{E(\mathbf{I})^2},$$

$$C = \frac{E[\mathbf{I}^2] - E[\mathbf{I}]^2}{E[\mathbf{I}]^2}. \tag{38}$$

Expanding $E[\mathbf{I}]$, we obtain

$$E[\mathbf{I}] = E[\rho\lambda(l_x\mathbf{n}_x + l_y\mathbf{n}_y + l_z\mathbf{n}_z)],$$

$$E[\mathbf{I}] = \rho\lambda\{l_xE[\mathbf{n}_x] + l_yE[\mathbf{n}_y] + l_zE[\mathbf{n}_z]\}. \tag{39}$$

As $E[\mathbf{n}_x]$ and $E[\mathbf{n}_y]$ both equal zero, we have

$$E[\mathbf{I}] = \rho\lambda l_zE[\mathbf{n}_z]. \tag{40}$$

For $E[\mathbf{I}^2]$, we have

$$E[\mathbf{I}^2] = E[\rho^2\lambda^2(l_x\mathbf{n}_x + l_y\mathbf{n}_y + l_z\mathbf{n}_z)^2],$$

$$E[\mathbf{I}^2] = \rho^2\lambda^2\{l_x{}^2E[\mathbf{n}_x{}^2] + l_y{}^2E[\mathbf{n}_y{}^2] + l_z{}^2E[\mathbf{n}_z{}^2] + 2l_xl_yE[\mathbf{n}_x\mathbf{n}_y] + 2l_xl_zE[\mathbf{n}_x\mathbf{n}_z] + 2l_yl_zE[\mathbf{n}_y\mathbf{n}_z]\}. \tag{41}$$

The cross terms go to zero (Proposition A5), so we have

$$E[\mathbf{I}^2] = \rho^2\lambda^2\{l_x{}^2E[\mathbf{n}_x{}^2] + l_y{}^2E[\mathbf{n}_y{}^2] + l_z{}^2E[\mathbf{n}_z{}^2]\}. \tag{42}$$

$\mathbf{n}_x$ and $\mathbf{n}_y$ may be rewritten in terms of $\mathbf{n}_z$ and the tilt $\mathbf{T}$ as

$$\mathbf{n}_x = \sqrt{1 - \mathbf{n}_z{}^2}\cos\mathbf{T}, \tag{43}$$

$$\mathbf{n}_y = \sqrt{1 - \mathbf{n}_z{}^2}\sin\mathbf{T}, \tag{44}$$

and since $\mathbf{n}_z$ and $\mathbf{T}$ are independent for isotropic surface processes (Proposition A4), we can rewrite Eq. (42) as

$$E[\mathbf{I}^2] = \rho^2\lambda^2\{l_x{}^2E[1 - \mathbf{n}_z{}^2]E[\cos^2\mathbf{T}] + l_y{}^2E[1 - \mathbf{n}_z{}^2] \times E[\sin^2\mathbf{T}] + l_z{}^2E[\mathbf{n}_z{}^2]\}. \tag{45}$$

For isotropic surface processes, $\mathbf{T}$ is uniformly distributed over the interval $[0\text{–}2\pi)$ (Proposition A4), so that $E[\sin^2\mathbf{T}] = E[\cos^2\mathbf{T}] = 1/2$. Substituting into Eq. (45) and simplifying, we obtain

$$E[\mathbf{I}^2] = \tfrac{1}{2}\rho^2\lambda^2\{1 - l_z^2 + (3l_z^2 - 1)E[\mathbf{n}_z^2]\}. \quad (46)$$

Substituting Eqs. (40) and (46) into Eqs. (38), we obtain for luminance contrast

$$C = \frac{1 - l_z^2 + (3l_z^2 - 1)E[\mathbf{n}_z^2]}{2l_z^2 E[\mathbf{n}_z]^2} - 1. \quad (47)$$

$$E\left[\left(\frac{\partial \mathbf{n}_x}{\partial_y}\right)^2\right] = \left\{\frac{3}{4}E[\mathbf{n}_z^2] - \frac{1}{2}E[\mathbf{n}_z^4] + \frac{3}{4}E[\mathbf{n}_z^6]\right\}E[\mathbf{P}_y^2], \quad (54)$$

$$E\left[\left(\frac{\partial \mathbf{n}_z}{\partial x}\right)^2\right] = E\left[\left(\frac{\partial \mathbf{n}_z}{\partial y}\right)^2\right] = \{2E[\mathbf{n}_z^4] - 2E[\mathbf{n}_z^6]\}E[\mathbf{P}_y^2]. \quad (55)$$

Substituting into Eq. (52), we get

$$R = \frac{5E[\mathbf{n}_z^2] + 2E[\mathbf{n}_z^4] + 5E[\mathbf{n}_z^6] - l_z^2\{5E[\mathbf{n}_z^2] - 6E[\mathbf{n}_z^4] + 13E[\mathbf{n}_z^6]\}}{3E[\mathbf{n}_z^2] - 2E[\mathbf{n}_z^4] + 3E[\mathbf{n}_z^6] - l_z^2\{3E[\mathbf{n}_z^2] - 10E[\mathbf{n}_z^4] + 11E[\mathbf{n}_z^6]\}}. \quad (56)$$

This relation provides the first statistic for the estimator.

The second statistic that is to be used in the estimator uses the partial derivatives of image luminance. It is based on the observation that the variance of the derivative of luminance is greatest when computed along a direction parallel to the light-source tilt and is minimal when computed along an orthogonal direction (Section 3, Proposition 1). The ratio of the two variances depends only on l_z and some of the moments of $\mathbf{n}_z$. Our second statistic, then, is

$$R = \frac{E[(\partial \mathbf{I}/\partial x)^2]}{E[(\partial \mathbf{I}/\partial y)^2]}, \quad (48)$$

where x is taken to be in the direction of the illuminant tilt and y is in the orthogonal direction. The derivation of R is rather long and involves some cumbersome algebra, so only the main steps will be described here. The remaining details are given in Appendix B.

In the coordinate system that we have defined, the illuminant vector is given by $\vec{L} = (l_x, 0, l_z)^T$, and the derivative of luminance computed in an arbitrary direction θ is given by

$$\frac{\partial \mathbf{I}}{\partial r_\theta} = \rho\lambda\left(l_x \frac{\partial \mathbf{n}_x}{\partial r_\theta} + l_z \frac{\partial n_z}{\partial r_\theta}\right). \quad (49)$$

The variance of $\partial \mathbf{I}/\partial r_\theta$, given in Eq. (28), is

$$E\left[\left(\frac{\partial \mathbf{I}}{\partial r_\theta}\right)^2\right] = \rho^2\lambda^2\left\{l_x^2 E\left[\left(\frac{\partial \mathbf{n}_x}{\partial r_\theta}\right)^2\right] + l_z^2 E\left[\left(\frac{\partial \mathbf{n}_z}{\partial r_\theta}\right)^2\right]\right\}. \quad (50)$$

Replacing l_x with $\sqrt{(1 - l_z^2)}$, we get

$$E\left[\left(\frac{\partial \mathbf{I}}{\partial r_\theta}\right)^2\right] = \rho^2\lambda^2\left\{(1 - l_z^2)E\left[\left(\frac{\partial \mathbf{n}_x}{\partial r_\theta}\right)^2\right] + l_z^2 E\left[\left(\frac{\partial \mathbf{n}_z}{\partial r_\theta}\right)^2\right]\right\}. \quad (51)$$

Substituting Eq. (51) into Eq. (48), we obtain

$$R = \frac{(1 - l_z^2)E[(\partial \mathbf{n}_x/\partial x)^2] + l_z^2 E[(\partial \mathbf{n}_z/\partial x)^2]}{(1 - l_z^2)E[(\partial \mathbf{n}_x/\partial y)^2] + l_z^2 E[(\partial \mathbf{n}_z/\partial y)^2]}. \quad (52)$$

The only terms that differ between the numerator and the denominator are $E[(\partial \mathbf{n}_x/\partial x)^2]$ and $E[(\partial \mathbf{n}_x/\partial y)^2]$. Note that $E[(\partial \mathbf{n}_z/\partial x)^2] = E[(\partial \mathbf{n}_z/\partial y)^2]$. Expressions for the expectations in Eq. (52) are derived in Appendix B and summarized below:

$$E\left[\left(\frac{\partial \mathbf{n}_x}{\partial x}\right)^2\right] = \left\{\frac{5}{4}E[\mathbf{n}_z^2] + \frac{1}{2}E[\mathbf{n}_z^4] + \frac{5}{4}E[n_z^6]\right\}E[\mathbf{P}_y^2], \quad (53)$$

This relation provides the second statistic for the estimator.

All that is required for implementation of the estimator is a specification of the local distributions of the partial-derivative processes, $\mathbf{P}$ and $\mathbf{Q}$. The moments of $\mathbf{n}_z$ must then be expressed as functions of the standard deviation of $\mathbf{P}$ and $\mathbf{Q}$, $\sigma_p = \sigma_q$:

$$E[\mathbf{n}_z^i] = g_i(\sigma_p). \quad (57)$$

Substitution of the functions $g_i(\sigma_p)$ for the $E[\mathbf{n}_z^i]$ terms in Eqs. (47) and (56) gives equations that are functions of the two unknowns, l_z and σ_p. Measurements of R and C from a given image may then be used in the simultaneous solution of these equations to derive estimates of l_z and σ_p.

5. IMPLEMENTATION

This section describes an implementation of the slant estimator for surfaces whose depths have a Gaussian distribution (the tilt estimator is independent of the form of the distribution). The first step in the implementation is to derive the probability distribution of the z component of surface normals $\mathbf{n}_z$. The second step is to derive the functions $g_i(\sigma_p)$ for the ith moments of $\mathbf{n}_z$.

Define a new random process $\mathbf{R}$ as

$$\mathbf{R} = \sqrt{\mathbf{P}^2 + \mathbf{Q}^2}. \quad (58)$$

$\mathbf{R}$ is the length of the gradient vector of $\mathbf{S}$. $\mathbf{P}$ and $\mathbf{Q}$ are both Gaussian with equal variance σ_p^2, and $\mathbf{R}$ can be shown to have a Rayleigh distribution

$$f_{\mathbf{R}}(r) = p(\mathbf{R} = r) = \frac{r}{\sigma_p^2}\exp[-r^2/(2\sigma_p^2)] \qquad (r \geq 0). \quad (59)$$

The z component of the surface normal is given by

$$\mathbf{n}_z = g(\mathbf{R}) = \frac{1}{\sqrt{\mathbf{R}^2 + 1}}. \quad (60)$$

$\mathbf{n}_z$ is a strictly monotonic, decreasing function of $\mathbf{R}$, so that its probability distribution is related to $f_{\mathbf{R}}(r)$ by

$$f_{\mathbf{n}_z}(n_z) = f_{\mathbf{R}}[g^{-1}(n_z)]\left|\frac{dg^{-1}(n_z)}{dn_z}\right|. \quad (61)$$

The resulting distribution is given by

$$f_{\mathbf{n}_z}(n_z) = \frac{\exp[1/(2\sigma_p^2)]}{\sigma_p^2 n_z^3}\exp[-1/(2n_z^2\sigma_p^2)] \qquad (0 < n_z \leq 1). \quad (62)$$

We require functional relations between the first, second, fourth, and sixth moments of $\mathbf{n}_z$ and σ_p. These relations are given below. Appendix C contains further details of their derivation:

$$E[\mathbf{n}_z] = \frac{\sqrt{2}\pi}{2\sigma_p} \exp[1/(2\sigma_p{}^2)]\left[1 - \mathrm{erf}\left(\frac{1}{\sqrt{2}\sigma_p}\right)\right], \quad (63)$$

$$E[\mathbf{n}_z{}^2] = \frac{\exp[1/(2\sigma_p{}^2)]}{2\sigma_p{}^2} E_1\left(\frac{1}{2\sigma_p{}^2}\right), \quad (64)$$

$$E[\mathbf{n}_z{}^4] = \frac{1}{2\sigma_p{}^2}(1 - E[\mathbf{n}_z{}^2]), \quad (65)$$

$$E[\mathbf{n}_z{}^6] = \frac{1}{4\sigma_p{}^2}(1 - E[\mathbf{n}_z{}^4]). \quad (66)$$

In the equations above, erf( ) is the standard error function and E_1( ) is the first-order exponential integral (see Appendix C for definitions). Note that the fourth and sixth moments are given as recurrence relations. This simplifies the computations somewhat. Substitution of the moment functions into Eqs. (47) and (56) completes the implementation of the estimator. In the computer simulations, the special functions were replaced by standard polynomial approximations.[8]

6. SIMULATIONS

We applied the estimator to images of two different types of surface, randomly generated, smoothed fractal surfaces and spheres. A fractal model was used for one set of test surfaces because it provided a mechanism for the random generation of naturalistic surfaces. We varied the degree of relief in these surfaces by scaling the depths along the viewer axis. Spheres were used as a second test surface for two reasons. First, they are prototypical examples of isotropic surfaces, and as such they provide a test of the best possible performance of the tilt estimator. Second, they are atypical examples of surfaces drawn from a Gaussian ensemble, so that they provide a test of the generalizability of the implementation of the slant estimator. Examples of the test images that were used are shown in Fig. 4.

The size of the images that were used for the simulations was 256 × 256 pixels. The partial derivatives of luminance were calculated using a seven-point discrete derivative filter, the kernel of which is given by

$$\mathbf{D} = (-0.0577, 0.215, -0.804, 0, 0.804, -0.215, 0.0577)^T. \quad (67)$$

This operation gave better results than a simple discrete differencing operation. For the images of smoothed fractal surfaces, the required image statistics were calculated by using the entire image; but for the images of the spheres, only points within the occluding contour of the spheres were used. This was done to avoid the biasing effects of the relatively large values calculated for the partial derivatives at the spheres' boundaries.

Illuminant tilt was estimated by using Eq. (24). For the estimation of illuminant slant and orientation variance, we define an error functional that incorporates the squared differences between measured and computed values of C and R. The error functional is given by

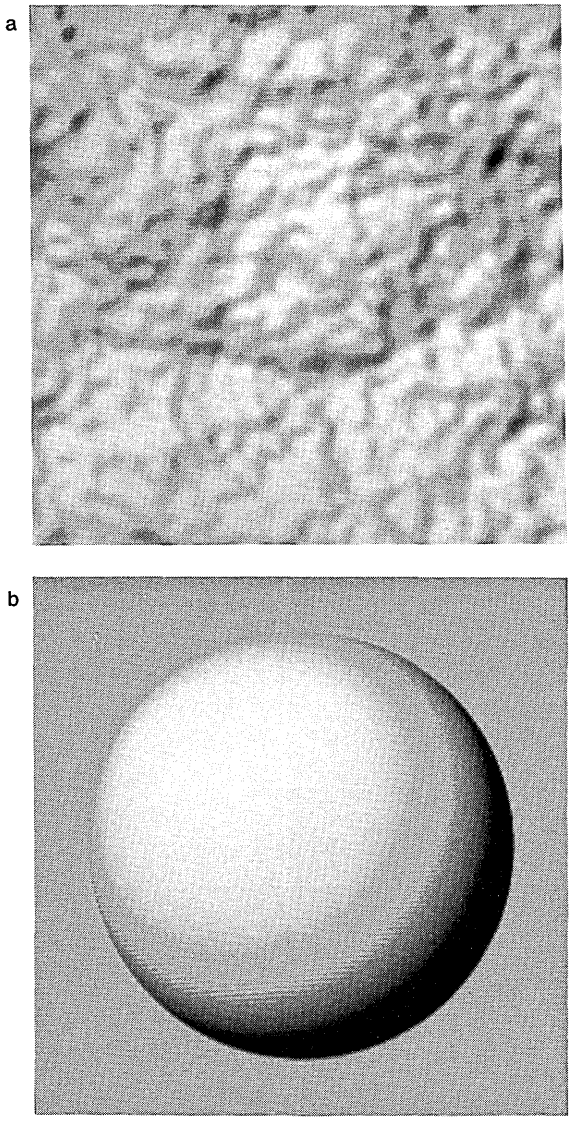

Fig. 4. Images used as examples in the simulations. a, The first test image is a smoothed fractal surface. b, The second test image, a sphere, is shown. Both images are generated by using a point light source at 135° tilt and 30° slant.

$$E(\hat{l}_z, \hat{\sigma}_p) = [C_m - C(\hat{l}_z, \hat{\sigma}_p)]^2 + [R_m - R(\hat{l}_z, \hat{\sigma}_p)]^2, \quad (68)$$

where C_m and R_m are the values of C and R that are measured from an image and $C(\hat{l}_z, \hat{\sigma}_p)$ and $R(\hat{l}_z, \hat{\sigma}_p)$ are the values that are computed by using Eqs. (47), (56), and (63)–(66). Simulations indicated that this error functional was convex for images of the types of surfaces used here; therefore we used a simple coarse-to-fine-resolution search of the (l_z, σ_p) parameter space to find the minimum of the error function. The estimated illuminant slant is calculated from $\hat{l}_z$ using Eq. (8).

The first two simulations were designed to analyze the performance of the tilt estimator. The third and fourth simulations provided data on the performance of the slant and surface-relief estimator.

Simulation 1

In the first simulation, the illuminant slant was held fixed at 30°, and seven different tilts between 0° and 90° were used

Table 1. Tilt Estimates for Smoothed Fractal Surfaces: Simulation 1[a]

Illuminant Tilt (τ_l)	Estimated Tilt ($\hat{\tau}_l \pm \sigma_{\hat{\tau}_l}$)	N
0.0	0.70 ± 4.52	40
15.0	16.05 ± 5.80	40
30.0	30.60 ± 4.53	40
45.0	44.85 ± 5.65	40
60.0	60.50 ± 6.56	40
75.0	75.72 ± 5.71	40
90.0	88.55 ± 4.94	40

[a] Estimated illuminant tilt for images of smoothed fractal surfaces illuminated from seven different tilts and a slant of 30°.

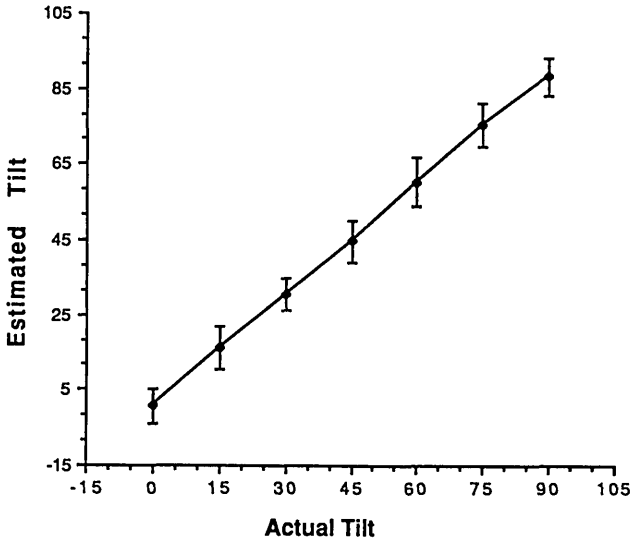

Fig. 5. Plot of the average estimated illuminant tilt generated by the tilt estimator, when applied to images of smoothed fractal surfaces, versus the actual illuminant tilt. The error bars represent the standard deviation of the estimates (Table 2).

Table 2. Tilt Estimates for Spheres: Simulation 1[a]

Illuminant Tilt (τ_l)	Estimated Tilt ($\hat{\tau}_l$)	N
0.0	1.0	1
15.0	15.9	1
30.0	31.5	1
45.0	45.0	1
60.0	58.5	1
75.0	74.1	1
90.0	89.0	1

[a] Estimated illuminant tilt for images of spheres illuminated from seven different tilts and a slant of 30°.

to generate test images of smoothed fractal surfaces and spheres. Table 1 summarizes the performance of the tilt estimator for the images of randomly generated fractal surfaces. The standard deviation of the tilt estimates is approximately 5°, which indicates the accuracy of the estimator. Figure 5 shows a plot of this data, with the standard deviation of the tilt estimates shown as error bars. Table 2 shows the tilt estimates for the images of spheres. The estimator is near perfect for these images, with errors ranging from 0° at a tilt of 45° to 1.5° at tilts of 30° and 60°. This performance should be expected, however, as spheres are prototypical examples of isotropic surfaces.

The estimator shows a small bias toward 45° for the images of spheres. This bias is probably due to the effect of discretization on the calculation of the partial derivatives at the boundary of the shadowed region of the sphere. No such apparent bias can be seen in the performance of the estimator for the images of fractal surfaces.

Simulation 2

The second simulation was designed to study the effect of illuminant slant on the performance of the tilt estimator. Test images for this simulation were generated using a fixed illuminant tilt of 45° and nine different illuminant slants that varied between 0° and 40° (illuminant tilt is actually indeterminate for a slant of 0°).

The performance of the estimator on the images of smoothed fractal surfaces was highly dependent on illuminant slant (Table 3). Figure 6 is a plot of the standard deviation of the tilt estimate as a function of illuminant

Table 3. Tilt Estimates for Smoothed Fractal Surfaces: Simulation 2[a]

Illuminant Slant (s_l)	Estimated Tilt ($\hat{\tau}_l \pm \sigma_{\hat{\tau}_l}$) $\tau_l = 45.0$	N
0.0	48.35 ± 51.89	40
5.0	42.77 ± 44.62	40
10.0	47.05 ± 23.89	40
15.0	43.62 ± 11.78	40
20.0	40.85 ± 12.23	40
25.0	43.47 ± 6.51	40
30.0	43.97 ± 5.61	40
35.0	44.72 ± 4.22	40
40.0	44.15 ± 4.21	40

[a] Estimated illuminant tilt for images of smoothed fractal surfaces illuminated from a fixed tilt of 45° and nine different slants.

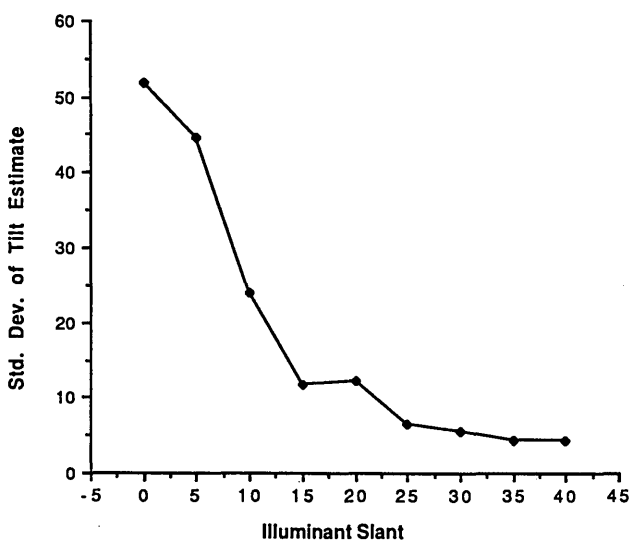

Fig. 6. Plot of the standard deviation of estimated illuminant tilt generated by the tilt estimator, when applied to images of smoothed fractal surfaces, versus the illuminant slant used in generating the images.

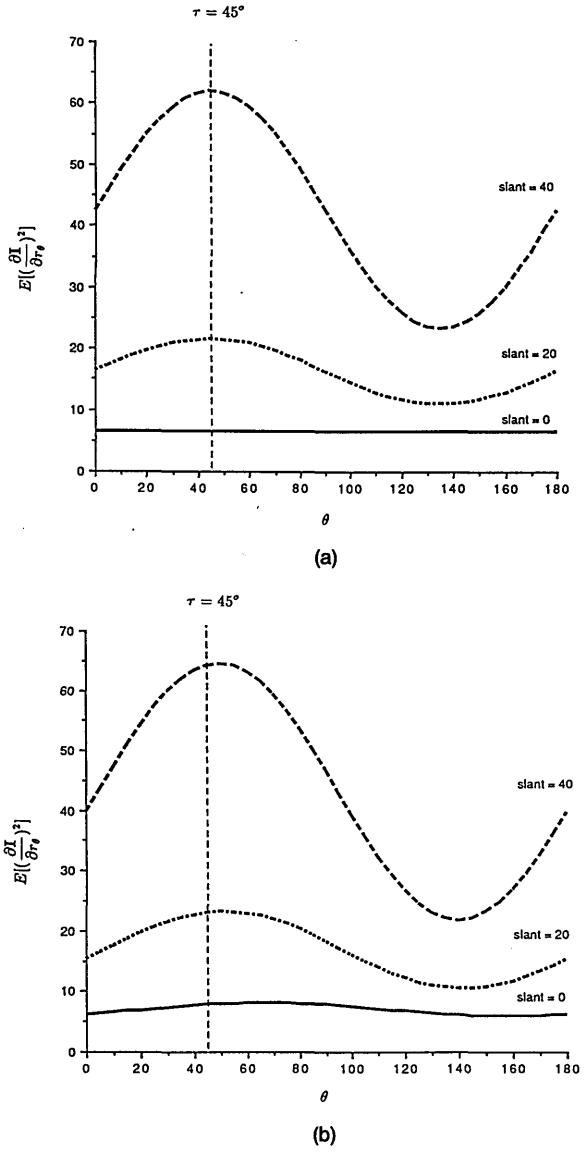

Fig. 7. a, Plot of the variance of the partial derivative of luminance as a function of the direction in which the derivative is computed for images of smoothed fractal surfaces. The images are generated by using a light source at a tilt of 45° and slants of 0°, 20°, and 40°. These data reflect an ensemble average, and, as expected, the peak of the function is found at 45° (see text for discussion). b, Plot of the sample variance as a function of direction for images of a sample fractal surface. The peaks of the functions are shifted away from 45° owing to random variations of the surface. Note that the accuracy of the peak is highest for the images generated with larger slants.

slant. It drops from a value of 51.9 for 0° slant to an asymptotic lower value of 4.0 for 40° slant. The decrease in error with increasing illuminant slant results from the increasing likelihood that anisotropies in the luminance distribution that were caused by a slanted illuminant outweigh those anisotropies that were caused by random variation in sample surfaces (e.g., a given surface may have a large ridge running in one direction). This decrease in error is illustrated in Fig. 7, which shows plots of $E[(\partial \mathbf{I}/\partial r_\theta)^2]$ as a function of θ for three classes of image. The classes correspond to images of smoothed fractal surfaces illuminated by light sources with slants of 0°, 20°, and 40°. The peakedness of the variance function indicates the sensitivity of the estimator to random variations of a surface. When the illuminant slant is 0°, the function is flat, which reflects the fact that the tilt is indeterminate. In this case, the estimated tilt is completely determined by the random surface variations. As the slant is increased, the peak of the function becomes more pronounced, and the estimator becomes less sensitive to random surface variations.

Table 4 shows that the tilt estimator is perfect for each of the images of spheres that are used in this simulation.

Simulation 3

We applied the illuminant slant and surface-relief estimator to images of smoothed fractal surfaces that were generated using seven different illuminant slants between 0° and 30°. The tilt of the illuminant was held fixed at 45°, but an estimate of tilt that was obtained from the tilt estimator was used in place of the actual tilt in the estimation of slant and degree of relief. Images of 100 different surfaces were generated for each slant. The sample standard deviation of surface orientation, σ_p, was distributed fairly uniformly between 0.20 and 0.62.

Table 5 summarizes the performance of the estimator for each of the seven illuminant slants. The bias in the slant estimate drops from 6.24° to 0.68° as the illuminant slant

Table 4. Tilt Estimates for Spheres: Simulation 2[a]

Illuminant Slant (s_l)	Estimated Tilt ($\hat{\tau}_l$) $\tau_l = 45.0$	N
0.0	—	1
5.0	45.0	1
10.0	45.0	1
15.0	45.0	1
20.0	45.0	1
25.0	45.0	1
30.0	45.0	1
35.0	45.0	1
40.0	45.0	1

[a] Estimated illuminant tilt for images of spheres illuminated from a fixed tilt of 45° and nine different slants.

Table 5. Tilt Estimates for Smoothed Fractal Surfaces: Simulation 3[a]

Illuminant Slant (s_l)	Estimated Slant ($\hat{s}_l \pm \sigma_{\hat{s}_l}$)	Error in Estimated Degree of Relief $[(\hat{\sigma}_p - \sigma_p)^2]$	N
0.0	6.24 ± 3.58	0.0032	100
5.0	7.25 ± 3.69	0.0034	100
10.0	11.46 ± 3.30	0.0021	100
15.0	16.40 ± 3.31	0.0017	100
20.0	21.60 ± 3.11	0.0021	100
25.0	26.13 ± 3.26	0.0017	100
30.0	30.68 ± 3.28	0.0016	100

[a] Estimated illuminant slant and the error in the estimated degree of surface relief for images of smoothed fractal surfaces illuminated from a fixed tilt of 45° and seven different slants. The third column lists the average error between the sample standard deviation of surface orientation for a surface and the estimated standard deviation.

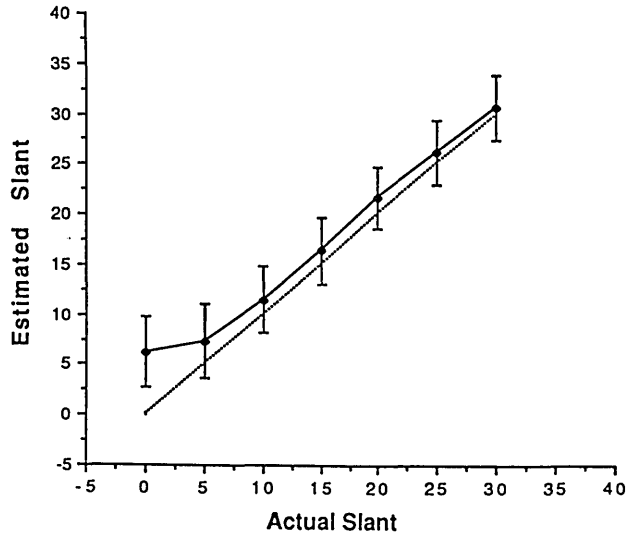

Fig. 8. Plot of the average estimated illuminant slant generated by the slant and surface-relief estimator, when applied to images of smoothed fractal surfaces, versus the actual illuminant slant. The error bars represent the standard deviation of the estimates (Table 5). The ideal performance is shown as a dotted line.

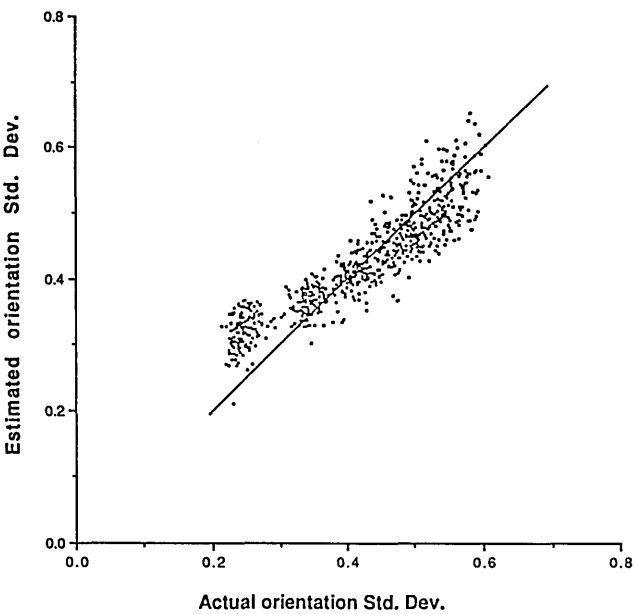

Fig. 9. Scatter plot of the estimated standard deviation of **P** and **Q** ($\hat{\sigma}_n$) generated by the slant and surface-relief estimator, when applied to images of smoothed fractal surfaces, versus the actual standard deviation (σ_p). The ideal performance is shown as a solid line.

increases from 0° to 30°. The standard deviation of the estimates remains essentially constant around 3.5° for each of the illuminant slants. These data are plotted in Fig. 8. The average mean-squared error in the estimate of σ_p decreases from 0.0032 at 0° slant to 0.0016 at 30° slant, which shows a small improvement in the accuracy of the estimate of degree of surface relief with increased illuminant slant. Figure 9 shows a scatter plot of the estimated values of σ_p versus the actual values for all 700 images tested. Note that the apparent slope of the plot is somewhat less than 1, which indicates that the estimator is positively biased for surfaces with $\sigma_p < 0.45$ and negatively biased for surfaces with $\sigma_p > 0.45$.

Simulation 4

In the last simulation, we applied the estimator to images of spheres that were illuminated from the same seven slants that were used in Simulation 3. The tilt of the illuminant was held fixed at 45°. Again, we used the estimated tilt for the simulation; however, as shown in Table 4, this estimate was equivalent to the real tilt. Table 6 summarizes the results of this simulation. The estimator overestimates the illuminant slant in all cases, with the error increasing from 6.25° at 0° slant to 13.76° at 30° slant. The estimator underestimates the value of σ_p, which should be 1.81, with an error that increases from −0.5 at 0° slant to −1.22 at 30° slant.

7. DISCUSSION

The estimators show a number of regular properties in their performance. The accuracy of the tilt estimate is, in general, a function of the slant of the illuminant; accuracy improves with increasing illuminant slant. As described above, this improvement is a direct result of the estimator's dependence on the isotropy of the projected surface. It can be tricked by anisotropies in the luminance distribution that are caused by random anisotropies in a surface. The sensitivity of the estimator to these random variations decreases with increasing illuminant slant, which leads to improved performance in these conditions. The analysis illustrated in Fig. 7 can be extended to include noise in the imaging system. As with its sensitivity to random surface variations, the estimator's sensitivity to noise decreases with increasing illuminant slant. We emphasize the point that the tilt estimator is based on a minimal set of assumptions about imaged surfaces. Further improvement of the estimator would require the extraction of some, possibly very general, shape information from the image.

The slant and surface-relief estimator, as it was implemented for Gaussian surfaces, performs well on images of smoothed fractal surfaces; however, it does not seem to generalize well to images of spheres. Though this problem is partially due to the innapropriateness of the Gaussian distribution for modeling spherical surfaces, it is primarily due to the pervasive presence of self-shadowing in the images of the

Table 6. Tilt Estimates for Spheres: Simulation 4[a]

Illuminant Slant (s_l)	Estimated Slant ($\hat{s}_l$)	Estimated Degree of Relief ($\hat{\sigma}_p$) $\sigma_p = 1.81$	N
0.0	6.25	1.31	1
5.0	8.77	1.25	1
10.0	16.86	1.03	1
15.0	23.96	0.89	1
20.0	30.54	0.77	1
25.0	37.19	0.67	1
30.0	43.76	0.59	1

[a] Estimated illuminant slant and degree of surface relief for images of spheres illuminated from a fixed tilt of 45° and seven different slants. The third column lists the estimated standard deviation of surface orientation, which is to be compared with the real standard deviation of 1.81.

spheres. The effect of self-shadowing is clearly seen in the pattern of results in Table 6. As illuminant slant increases, putting more of the sphere in shadow, the estimator error increases. The effect of self-shadowing was not evident in the results from the simulations with smoothed fractal surfaces, because shadows appeared only in images of those surfaces with the greatest degree of relief, and then only covered a small proportion of an image.

Self-shadowing is probably the single largest problem facing an estimator that makes use of global image statistics. Shadows bias the sample statistics, particularly at sharp boundaries, where the abnormally large derivatives dominate the calculated expectations. It is hard to see a way to deal with this problem efficiently when attempting to use only global image statistics for the estimator. One could, of course, attempt to detect shadows before applying the estimator and include only those regions of the image that are not in shadow in the statistics. Even if this were feasible, it would introduce a bias into the sampling, which would give preference to regions in the image that correspond to regions of the surface that face the illuminant.

The problem seems to contradict our intuitions about human perception because shadows actually seem to help us in estimating illuminant direction. A full account of human perception of illuminant direction must not only avoid the problems that are posed by the presence of shadows in images but actually make use of the information available in the shadows.

8. SUMMARY

Previous models for estimating illuminant direction are based on the limiting assumption that the distribution of surface orientations in an image match those of a sphere. We derive an estimator for illuminant tilt that is based on a minimal set of assumptions that do not include the form of the distribution of surface orientations. We also develop a general format for an estimator of illuminant slant and degree of surface relief that is based on the same assumptions. Actual implementation of the slant and surface-relief estimator requires the specification of the form of the distribution of surface orientations.

APPENDIX A

If a two-dimensional stochastic process is mean-square differentiable, the mean and correlation functions of the mean-square partial derivatives are simply related to those of the original process. In this appendix, we present a summary of these relations and use them to prove some properties of the local correlations between a process and its mean-square partial derivatives and between the partial derivatives themselves. We will also prove some properties of the tilt and slant of $\mathbf{S}$ and of the process's normal vectors and their partial derivatives. These preliminaries are necessary for the derivation of the illuminant tilt and slant estimators.

Let $\mathbf{S}$ be a two-dimensional, wide-sense stationary stochastic process. We can write its correlation function as a function of the vector distance between points (x, y):

$$R_s(x, y) = E[\mathbf{S}(x, y)\mathbf{S}(0, 0)] = E[\mathbf{S}(x_0 + x, y_0 + y)\mathbf{S}(x_0, y_0)]. \quad \text{(A1)}$$

Let us assume that $\mathbf{S}$ is twice mean-square differentiable, so that we can define processes for its partial derivatives. Using the notation introduced in Section 2 of this paper, these processes are $\mathbf{P}$, $\mathbf{Q}$, $\mathbf{P}_x$, $\mathbf{P}_y$, $\mathbf{Q}_x$, and $\mathbf{Q}_y(\mathbf{P}_y = \mathbf{Q}_x)$. Derivation of the mean and correlation functions of the partial-derivative processes of $\mathbf{S}$ is a straightforward extension of the derivations for one-dimensional processes (see Ref. 9), and only the final results will be presented here.

The means of the partial-derivative processes are zero:

$$E[\mathbf{P}] = E[\mathbf{Q}] = E[\mathbf{P}_x] = E[\mathbf{P}_y] = E[\mathbf{Q}_x] = E[\mathbf{Q}_y] = 0. \quad \text{(A2)}$$

The correlation functions are obtained by appropriate differentiation of the correlation function of $\mathbf{S}$:

$$R_p(x, y) = -\frac{\partial^2}{\partial x^2} R_s(x, y), \quad \text{(A3)}$$

$$R_q(x, y) = -\frac{\partial^2}{\partial y^2} R_s(x, y), \quad \text{(A4)}$$

$$R_{p_x}(x, y) = \frac{\partial^4}{\partial x^4} R_s(x, y), \quad \text{(A5)}$$

$$R_{q_y}(x, y) = \frac{\partial^4}{\partial y^4} R_s(x, y), \quad \text{(A6)}$$

$$R_{p_y}(x, y) = R_{q_x}(x, y) = \frac{\partial^4}{\partial x^2 \partial y^2} R_s(x, y). \quad \text{(A7)}$$

The cross-correlation functions between $\mathbf{S}$ and its partial-derivative processes and between the partial-derivative processes themselves are given by

$$R_{sp}(x, y) = \frac{\partial}{\partial x} R_s(x, y), \quad \text{(A8)}$$

$$R_{sq}(x, y) = \frac{\partial}{\partial y} R_s(x, y), \quad \text{(A9)}$$

$$R_{pq}(x, y) = -\frac{\partial^2}{\partial x \partial y} R_s(x, y), \quad \text{(A10)}$$

$$R_{pp_x}(x, y) = -\frac{\partial^3}{\partial x^3} R_s(x, y), \quad \text{(A11)}$$

$$R_{qq_y}(x, y) = -\frac{\partial^3}{\partial y^3} R_s(x, y), \quad \text{(A12)}$$

$$R_{pp_y}(x, y) = -\frac{\partial^3}{\partial x^2 \mathrm{d}y} R_s(x, y), \quad \text{(A13)}$$

$$R_{qq_x}(x, y) = \frac{\partial^3}{\partial x \partial y^2} R_s(x, y), \quad \text{(A14)}$$

$$R_{p_x p_y}(x, y) = \frac{\partial^4}{\partial x^3 \partial y} R_s(x, y), \quad \text{(A15)}$$

$$R_{q_x q_y}(x, y) = \frac{\partial^4}{\partial x \partial y^3} R_s(x, y). \quad \text{(A16)}$$

We now consider the local correlations between the process $\mathbf{S}$ and its partial-derivative processes, that is, the correlations between the process and its partial derivatives that are evaluated at the same point. In doing so, we will limit

consideration to processes whose probability laws are invariant over rotations of the coordinate systems in which they are defined. We refer to this property of the processes as strict isotropy, a formal definition of which is given below.

Definition
A two-dimensional stochastic process **S** is strictly isotropic if, for any positions $(x_1, y_1), \ldots, (x_k, y_k)$ and all $k = 1, 2, 3, \ldots$, its kth-order density functions satisfy the condition

$$f_s[s(x_1, y_1), \ldots, s(x_k, y_k)] = f_s[s(x'_1, y'_1), \ldots, s(x'_k, y'_k)], \tag{A17}$$

where

$$x'_i = x_i \cos\theta + y_i \sin\theta, \tag{A18}$$

$$y'_i = -x_i \sin\theta + y_i \cos\theta \tag{A19}$$

for all θ, $0 \le \theta < 2\pi$, and all i, $1 \le i \le k$.

A wide-sense stationary process **S** is locally uncorrelated with its mean-square partial-derivative processes. If **S** is also strictly isotropic, then the partial-derivative processes are themselves locally uncorrelated. These two facts are stated and proved in the next two propositions.

Proposition A1
Let **S** be a wide-sense stationary, two-dimensional stochastic process. Let **S** be twice mean-square differentiable. The first mean-square partial-derivative processes are uncorrelated with the process **S** at the point at which they are evaluated. The first partial-derivative processes are uncorrelated with their derivative processes, the second mean-square partial derivatives of **S**, when evaluated at the same point. This gives the following relations:

$$E[\mathbf{SP}] = R_{sp}(0, 0) = 0, \tag{A20}$$

$$E[\mathbf{SQ}] = R_{sq}(0, 0) = 0, \tag{A21}$$

$$E[\mathbf{PP}_x] = R_{pp_x}(0, 0) = 0, \tag{A22}$$

$$E[\mathbf{PP}_y] = R_{pp_y}(0, 0) = 0, \tag{A23}$$

$$E[\mathbf{QQ}_x] = R_{qq_x}(0, 0) = 0, \tag{A24}$$

$$E[\mathbf{QQ}_y] = R_{qq_y}(0, 0) = 0. \tag{A25}$$

Proof
For a wide-sense stationary process, we have from Eq. (A8)

$$R_{sp}(x, y) = \frac{\partial}{\partial x} R_s(x, y).$$

Because it is wide-sense stationary, the correlation function of **S** obeys the relation

$$R_s(x, y) = R_s(-x, y).$$

Since $R_s(x, y)$ is differentiable, this relation implies that

$$R_{sp}(0, 0) = \frac{\partial}{\partial x} R_s(x, y)\big|_{x=0, y=0} = 0.$$

The other relations follow immediately, since the partial-derivative processes of a wide-sense stationary process are themselves wide-sense stationary.
Q.E.D.

Proposition A2
Let S be a wide-sense stationary, strictly isotropic, two-dimensional, stochastic process. Let **S** be twice mean-square differentiable. The first mean-square partial-derivative processes, **P** and **Q**, when evaluated at the same point, are uncorrelated. The second directional derivatives, $\mathbf{P}_x$ and $\mathbf{Q}_y$, and the second mixed derivative, $\mathbf{P}_y = \mathbf{Q}_x$, when evaluated at the same point, are uncorrelated. This gives the following relations:

$$E[\mathbf{PQ}] = R_{pq}(0, 0) = 0, \tag{A26}$$

$$E[\mathbf{P}_x\mathbf{P}_y] = E[\mathbf{P}_x\mathbf{Q}_x] = R_{p_xp_y}(0, 0) = 0, \tag{A27}$$

$$E[\mathbf{Q}_x\mathbf{Q}_y] = E[\mathbf{P}_y\mathbf{Q}_y] = R_{q_xq_y}(0, 0) = 0. \tag{A28}$$

Proof

We will show the proof only for the first relation, as all the proofs follow exactly the same form. It is convenient for the proof to make use of the power spectrum of S. The power spectrum is given by the Fourier transform $F_s(f_x, f_y)$ of the covariance function, where f_x and f_y are the two-dimensional frequency components. We have for the covariance function

$$R_s(x, y) = \int_{-\infty}^{\infty}\int_{-\infty}^{\infty} F_s(f_x, f_y)\exp(i2\pi f_x x)\exp(i2\pi f_y y)\mathrm{d}f_x\mathrm{d}f_y.$$

The cross correlation between **P** and **Q** is given by

$$R_{pq}(x, y) = \frac{\partial^2}{\partial x \partial y} R_s(x, y),$$

so we have

$$R_{pq}(x, y) = -\frac{\partial^2}{\partial x \partial y}\int_{-\infty}^{\infty}\int_{-\infty}^{\infty} F_s(f_x, f_y)\exp(i2\pi f_x x) \times \exp(i2\pi f_y y)\mathrm{d}f_x\mathrm{d}f_y,$$

$$R_{pq}(0, 0) \sim \int_{-\infty}^{\infty}\int_{-\infty}^{\infty} f_x f_y F_s(f_x, f_y)\mathrm{d}f_x\mathrm{d}f_y.$$

This is the center of mass of the power spectrum, $F_s(f_x, f_y)$. Since **S** is isotropic, its power spectrum is radially symmetric and has its center of mass at 0; therefore

$$R_{pq}(0, 0) = 0.$$

Carrying through the same calculation for the other cross correlations, we always obtain odd powers of f_x and f_y in the integral term, so that the integral equals 0 for these as well.
Q.E.D.

We can derive an invariant relationship between the variance of the second directional derivatives and the second mixed derivatives of wide-sense stationary, isotropic processes. The ratio of the variance of any second directional derivative to the second mixed derivative is equivalently 3. This is stated formally in Proposition A3.

Proposition A3
Let **S** be a wide-sense stationary, strictly isotropic, two-dimensional, stochastic process. Let **S** be twice mean-square differentiable. The variances of the second mean-square partial-derivative processes are related by

$$E[\mathbf{P}_x^2] = E[\mathbf{Q}_y^2] = 3E[\mathbf{P}_y^2] = 3E[\mathbf{Q}_x^2].$$

Proof
As in the proof of Proposition B2, we will derive terms for the correlation functions of the second partial-derivative processes that are evaluated at $x = 0, y = 0$ by using the power spectrum of **S**. For $\mathbf{P}_x$, we have

$$R_{p_x}(x, y) = \frac{\partial^4}{\partial x^4} R_s(x, y).$$

Writing $R_s(x, y)$ as the inverse Fourier transform of the power spectrum $F_s(f_x, f_y)$, we have

$$R_{p_x}(x, y) = \frac{\partial^4}{\partial x^4} \int_{-\infty}^{\infty} \int_{-\infty}^{\infty} F_s(f_x, f_y) \exp(i2\pi f_x x) \times \exp(i2\pi f_y y)\, df_x\, df_y,$$

$$R_{p_x}(x, y) = \int_{-\infty}^{\infty} \int_{-\infty}^{\infty} 16\pi^4 f_x^4 F_s(f_x, f_y) \exp(i2\pi f_x x) \times \exp(i2\pi f_y y)\, df_x\, df_y.$$

The variance of $\mathbf{P}_x$ is given by

$$E[\mathbf{P}_x^2] = R_{p_x}(0, 0) = \int_{-\infty}^{\infty} \int_{-\infty}^{\infty} 16\pi^4 f_x^4 F_s(f_x, f_y) df_x df_y.$$

The variances of the other second partial-derivative processes may be expressed in the same way, which gives

$$E[\mathbf{Q}_y^2] = R_{q_y}(0, 0) = \int_{-\infty}^{\infty} \int_{-\infty}^{\infty} 16\pi^4 f_y^4 F_s(f_x, f_y) df_x df_y,$$

$$E[\mathbf{P}_y^2] = E[\mathbf{Q}_x^2] = R_{p_y}(0, 0) = \int_{-\infty}^{\infty} \int_{-\infty}^{\infty} 16\pi^4 f_x^2 f_y^2 F_s(f_x, f_y) df_x df_y.$$

Converting to polar coordinates, we get for the variances

$$R_{p_x}(0,0) = \int_0^{2\pi} \int_0^{\infty} 16\pi^4 f_r^5 \cos^4\theta\, F_s(f_r) df_r d\theta = \int_0^{2\pi} \cos^4\theta\, d\theta \int_0^{\infty} 16\pi^4 f_r^5 F_s(f_r) df_r = \frac{3\pi}{4} \int_0^{2\pi} 16\pi^4 f_r^5 F_s(f_r) df_r,$$

$$R_{q_y}(0, 0) = \int_0^{2\pi} \int_0^{\infty} 16\pi^4 f_r^5 \sin^4\theta\, F_s(f_r) df_r d\theta = \int_0^{2\pi} \sin^4\theta\, d\theta \int_0^{\infty} 16\pi^4 f_r^5 F_s(f_r) df_r = \frac{3\pi}{4} \int_0^{\infty} 16\pi^4 f_r^5 F_s(f_r) df_r,$$

$$R_{p_y}(0, 0) = \int_0^{2\pi} \int_0^{\infty} 16\pi^4 f_r^5 \sin^2\theta \cos^2\theta\, F_s(f_r) df_r d\theta = \int_0^{2\pi} \sin^2\theta \cos^2\theta\, d\theta \int_0^{\infty} 16\pi^4 f_r^5 F_s(f_r) df_r = \frac{\pi}{4} \int_0^{\infty} 16\pi^4 f_r^5 F_s(f_r) df_r.$$

The variances differ only in the multiplicative constant before the integral term. For $\mathbf{P}_x$ and $\mathbf{Q}_y$ the constant is $3\pi/4$. For $\mathbf{P}_y$ and $\mathbf{Q}_x$ it is $\pi/4$. The relationship between the variances immediately follows.
Q.E.D.

We now consider the other representations of surface orientation that are used in this paper. First, let us characterize the processes that correspond to the tilt and slant of a strictly isotropic process **S**. These processes are deterministic functions of the partial derivative processes. The tilt is given by

$$\mathbf{T} = \tan^{-1} \frac{\mathbf{Q}}{\mathbf{P}}, \tag{A29}$$

and the slant is given by

$$\mathbf{\Sigma} = \cos^{-1} \left(\frac{1}{\sqrt{\mathbf{P}^2 + \mathbf{Q}^2 + 1}} \right). \tag{A30}$$

An immediate consequence of the isotropy of **S** is that the tilt has a uniform first-order marginal probability distribution and is independent of the slant. This is stated and proved in the following proposition.

Proposition A4
Let **S** be a two-dimensional, wide-sense stationary, strictly isotropic, mean-square differentiable process. Let **T** be the tilt and **Σ** be the slant of the process **S** as defined above. The first-order marginal probability distribution of **T** is uniform:

$$p[\mathbf{T}(x, y) = \tau] = \frac{1}{2\pi}, \qquad 0 \le \tau < 2\pi, \tag{A31}$$

and the processes **T** and **Σ** are locally independent. The processes $\mathbf{n}_z$ and **T** are also locally independent, as $\mathbf{n}_z$ is a deterministic function of **Σ**.

Proof
Select a point (x, y) and rotate the coordinate system for **S** by an arbitrary angle θ around that point. If the tilt of **S** at (x, y) is τ in the original coordinate system, the tilt in the new coordinate system is given by $\tau' = \tau - \theta$. Because the probability law of **S** is invariant to rotations of the coordinate system, the probabilities of the two tilts τ and τ' are equal:

$$p(\mathbf{T} = \tau) = p(\mathbf{T} = \tau') = p(\mathbf{T} = \tau - \theta) \qquad 0 \le \theta < 2\pi.$$

Since θ was picked arbitrarily, the implication is that $p(\mathbf{T} = \tau')$ is a constant for all τ', thus proving the first part of the proposition.

The slant of S at (x, y) does not change with rotations of the coordinate system, so that the conditional probability of the slant given the tilt is constant for $\mathbf{T} = \tau$ and $\mathbf{T} = \tau'$:

$$p(\mathbf{\Sigma}|\mathbf{T} = \tau) = p(\mathbf{\Sigma}|\mathbf{T} = \tau') = p(\mathbf{\Sigma}|\mathbf{T} = \tau - \theta) \qquad 0 \le \theta < 2\pi.$$

Again, since θ was picked arbitrarily, the implication is that $p(\mathbf{\Sigma}|\mathbf{T} = \tau')$ is constant for all τ'. We have, therefore,

$$p(\mathbf{\Sigma}|\mathbf{T}) = p(\mathbf{\Sigma}),$$

and $\mathbf{T}$ and $\mathbf{\Sigma}$ are independent.
Q.E.D.

The third representation of surface orientation that is used in this paper is that of the surface normal and its elements' partial derivatives. The vector process that corresponds to the surface normal is $\tilde{\mathbf{N}} = (\mathbf{n}_x, \mathbf{n}_y, \mathbf{n}_z)^T$, as defined in Section 2 of this paper. Like the gradient vector $(\mathbf{P}, \mathbf{Q})^T$, the elements of the normal vector of an isotropic process $\mathbf{S}$ are locally uncorrelated.

Proposition A5
Let $\mathbf{S}$ be a two-dimensional, wide-sense stationary, strictly isotropic, mean-square differentiable process. Let $\tilde{\mathbf{N}} = (\mathbf{n}_x, \mathbf{n}_y, \mathbf{n}_z)^T$ be a vector process that represents the normals of $\mathbf{S}$. The elements of $\tilde{\mathbf{N}}$, when evaluated at the same point, are uncorrelated; that is,

$$E[\mathbf{n}_x\mathbf{n}_y] = E[\mathbf{n}_x\mathbf{n}_z] = E[\mathbf{n}_y\mathbf{n}_z] = 0. \tag{A32}$$

Proof
$\tilde{\mathbf{N}}$ is the normalization of the vector $(-\mathbf{P}, -\mathbf{Q}, 1)^T$, so that $\mathbf{n}_x$ and $\mathbf{n}_y$ have the same relative values as $\mathbf{P}$ and $\mathbf{Q}$. The multivariate distribution of $\mathbf{n}_x$ and $\mathbf{n}_y$, therefore, has the same symmetry as the distribution of $\mathbf{P}$ and $\mathbf{Q}$, and since $E[\mathbf{PQ}] = 0$, then $E[\mathbf{n}_x\mathbf{n}_y] = 0$, proving the first relation.

We can write $\mathbf{n}_z$ as a function of $\mathbf{n}_x$ and $\mathbf{n}_y$ as

$$\mathbf{n}_z = \sqrt{1 - (\mathbf{n}_x{}^2 + \mathbf{n}_y{}^2)}.$$

It takes on the same positive value for $\mathbf{n}_x = n_x$ and $\mathbf{n}_x = -n_x$ and similarly for $\mathbf{n}_y$. Since the distributions of $\mathbf{n}_x$ and $\mathbf{n}_y$ are symmetric around zero ($\mathbf{S}$ being wide-sense stationary), we have

$$p(\mathbf{n}_x, \mathbf{n}_z) = p(-\mathbf{n}_x, \mathbf{n}_z),$$
$$p(\mathbf{n}_y, \mathbf{n}_z) = p(-\mathbf{n}_y, \mathbf{n}_z),$$

so that

$$E[\mathbf{n}_x\mathbf{n}_z] = E[\mathbf{n}_y\mathbf{n}_z] = 0.$$

Q.E.D.

The derivations of the illuminant tilt and slant estimators require that the partial derivatives of the elements of the normal vector be locally uncorrelated. In order to prove this relation, we need the assumption that the second-order partial derivatives of $\mathbf{S}$ are independent of the first-order partial derivatives that are evaluated at the same point. Proposition A1 states that these partial derivatives are uncorrelated for wide-sense stationary, strictly isotropic prcoesses. This fact does not, in general, imply that they are independent. Independence will hold, of course, for Gaussian processes, as the partial derivatives of the process would also be Gaussian. The implementation of the slant estimator given in this paper does, in fact, assume a Gaussian probabilty law for $\mathbf{S}$.

With the independence assumption, we can state and prove the following propostion.

Proposition A6
Let $\mathbf{S}$ be a two-dimensional, wide-sense stationary, strictly isotropic, mean-square differentiable process. Assume that the second-order partial derivatives of $\mathbf{S}$, $\mathbf{P}_x$, $\mathbf{Q}_y$, and $\mathbf{P}_y$ are independent of the first-order partial derivatives $\mathbf{P}$ and $\mathbf{Q}$. The partial derivatives of $\mathbf{n}_x$ and $\mathbf{n}_y$ are locally uncorrelated with the partial derivative of $\mathbf{n}_z$ that is computed in the same direction. The partial derivatives of any one of the elements of $\tilde{\mathbf{N}}$, which are computed in the x and y directions, are locally uncorrelated. Writing the partial derivative that is computed in an arbitrary direction, θ, as $\partial/\partial r_\theta$, we get the first relation, which is given by

$$E\left[\frac{\partial \mathbf{n}_x}{\partial r_\theta}\frac{\partial \mathbf{n}_z}{\partial r_\theta}\right] = E\left[\frac{\partial \mathbf{n}_y}{\partial r_\theta}\frac{\partial \mathbf{n}_z}{\partial r_\theta}\right] = 0. \tag{A33}$$

The second relation is given by

$$E\left[\frac{\partial \mathbf{n}_x}{\partial x}\frac{\partial \mathbf{n}_x}{\partial y}\right] = E\left[\frac{\partial \mathbf{n}_y}{\partial x}\frac{\partial \mathbf{n}_y}{\partial y}\right] = E\left[\frac{\partial \mathbf{n}_z}{\partial x}\frac{\partial \mathbf{n}_z}{\partial y}\right] = 0. \tag{A34}$$

Proof
To prove any one of these relations, we can expand the partial derivatives of the elements of $\tilde{\mathbf{N}}$ in terms of $\mathbf{n}_z$, $\mathbf{T}$, and the partial derivatives of $\mathbf{P}$ and $\mathbf{Q}$ and show that the resulting expression evaluates to zero. As examples, we will present proofs for the relations appearing in the derivation of the tilt estimator given in Section 3 of this paper. The first of these is that $E[(\partial \mathbf{n}_x/\partial r_\theta)(\partial \mathbf{n}_z/\partial r_\theta)] = 0$. Expanding $\partial \mathbf{n}_x/\partial r_\theta$, we get

$$\begin{aligned}\frac{\partial \mathbf{n}_x}{\partial r_\theta} &= \frac{\partial \mathbf{n}_x}{\partial \mathbf{P}}\frac{\partial \mathbf{P}}{\partial r_\theta} + \frac{\partial \mathbf{n}_x}{\partial \mathbf{Q}}\frac{\partial \mathbf{Q}}{\partial r_\theta} \\ &= \left[\frac{-1}{(\mathbf{P}^2 + \mathbf{Q}^2 + 1)^{1/2}}\frac{\mathbf{P}^2}{(\mathbf{P}^2 + \mathbf{Q}^2 + 1)^{3/2}}\right]\mathbf{P}_{r_\theta} \\ &\quad + \left[\frac{\mathbf{PQ}}{(\mathbf{P}^2 + \mathbf{Q}^2 + 1)^{3/2}}\right]\mathbf{Q}_{r_\theta} \\ &= (-\mathbf{n}_z + \mathbf{n}_x{}^2\mathbf{n}_z)\mathbf{P}_{r_\theta} + (\mathbf{n}_x\mathbf{n}_y\mathbf{n}_z)\mathbf{Q}_{r_\theta}.\end{aligned} \tag{A35}$$

We can relate $\mathbf{n}_x$ and $\mathbf{n}_y$ to $\mathbf{n}_z$ and the tilt $\mathbf{T}$ by using

$$\mathbf{n}_x = \sqrt{1 - \mathbf{n}_z{}^2}\cos\mathbf{T}, \tag{A36}$$

$$\mathbf{n}_y = \sqrt{1 - \mathbf{n}_z{}^2}\sin\mathbf{T}. \tag{A37}$$

Substituting Eqs. (A36) and (A37) into Eq. (A35), we get

$$\begin{aligned}\frac{\partial \mathbf{n}_x}{\partial r_\theta} &= [-\mathbf{n}_z + (\mathbf{n}_z - \mathbf{n}_z{}^3)\cos^2\mathbf{T}]\mathbf{P}_{r_\theta} \\ &\quad + [(\mathbf{n}_z - \mathbf{n}_z{}^3)\sin\mathbf{T}\cos\mathbf{T}]\mathbf{Q}_{r_\theta}.\end{aligned} \tag{A38}$$

Expanding $\partial \mathbf{n}_z/\partial r_\theta$ in the same way, we get

$$\frac{\partial \mathbf{n}_z}{\partial r_\theta} = (\mathbf{n}_z{}^2\sqrt{1 - \mathbf{n}_z{}^2}\cos\mathbf{T})\mathbf{P}_{r_\theta} + (\mathbf{n}_z{}^2\sqrt{1 - \mathbf{n}_z{}^2}\sin\mathbf{T})\mathbf{Q}_{r_\theta}. \tag{A39}$$

The cross correlation between $\partial \mathbf{n}_x/\partial r_\theta$ and $\partial \mathbf{n}_z/\partial r_\theta$ is given by

$$E\left[\frac{\partial \mathbf{n}_x}{\partial r_\theta}\frac{\partial \mathbf{n}_z}{\partial r_\theta}\right] = E[-\mathbf{n}_z{}^3\sqrt{1-\mathbf{n}_z{}^2}\cos(\mathbf{T})\mathbf{P}_{r_\theta}{}^2]$$
$$+ E[\sqrt{1-\mathbf{n}_z{}^2}\,(\mathbf{n}_z{}^3-\mathbf{n}_z{}^5)\cos^3(\mathbf{T})\mathbf{P}_{r_\theta}{}^2]$$
$$+ E[\sqrt{1-\mathbf{n}_z{}^2}(\mathbf{n}_z{}^3-\mathbf{n}_z{}^5)\sin^2(\mathbf{T})\cos(\mathbf{T})\mathbf{Q}_{r_\theta}{}^2]$$
$$+ E[-\mathbf{n}_z{}^3\sqrt{1-\mathbf{n}_z{}^2}\sin(\mathbf{T})\mathbf{P}_{r_\theta}\mathbf{Q}_{r_\theta}]$$
$$+ 2E[\sqrt{1-\mathbf{n}_z{}^2}(\mathbf{n}_z{}^3-\mathbf{n}_z{}^5)\sin(\mathbf{T})\cos^2(\mathbf{T})\mathbf{P}_{r_\theta}\mathbf{Q}_{r_\theta}]. \quad \text{(A40)}$$

Because of the isotropy of $\mathbf{S}$, $\mathbf{n}_z$ and $\mathbf{T}$ are independent (Proposition A4), and since they may both be expressed as functions of $\mathbf{P}$ and $\mathbf{Q}$, they are also independent of $\mathbf{P}_{r_\theta}$ and $\mathbf{Q}_{r_\theta}$ (by assumption). The expectations of the terms that involve $\mathbf{n}_z$, $\mathbf{T}$, $\mathbf{P}_{r_\theta}$, and $\mathbf{Q}_{r_\theta}$ may, therefore, be separated, giving

$$E\left[\frac{\partial \mathbf{n}_x}{\partial r_\theta}\frac{\partial \mathbf{n}_z}{\partial r_\theta}\right] = E[-\mathbf{n}_z{}^3\sqrt{1-\mathbf{n}_z{}^2}]E[\cos\mathbf{T}]E[\mathbf{P}_{r_\theta}{}^2]$$
$$+ E[\sqrt{1-\mathbf{n}_z{}^2}(\mathbf{n}_z{}^3-\mathbf{n}_z{}^5)]E[\cos^3\mathbf{T}]E[\mathbf{P}_{r_\theta}{}^2]$$
$$+ E[\sqrt{1-\mathbf{n}_z{}^2}(\mathbf{n}_z{}^3-\mathbf{n}_z{}^5)]E[\sin^2\mathbf{T}\cos\mathbf{T}]E[\mathbf{Q}_{r_\theta}{}^2]$$
$$+ E[-\mathbf{n}_z{}^3\sqrt{1-\mathbf{n}_z{}^2}]E[\sin\mathbf{T}]E[\mathbf{P}_{r_\theta}\mathbf{Q}_{r_\theta}]$$
$$+ 2\,E[\sqrt{1-\mathbf{n}_z{}^2}(\mathbf{n}_z{}^3-\mathbf{n}_z{}^5)]E[\sin\mathbf{T}\cos^2\mathbf{T}]$$
$$\times E[\mathbf{P}_{r_\theta}\mathbf{Q}_{r_\theta}]. \quad \text{(A41)}$$

Since $\mathbf{T}$ has a uniform distribution, $E[\sin\mathbf{T}\cos^n\mathbf{T}] = E[\sin^n\mathbf{T}\cos\mathbf{T}] = 0$ for $n \geq 0$, and $E[\cos^m\mathbf{T}] = 0$, for m odd. The terms that involve $\mathbf{T}$, therefore, all go to zero, which leaves

$$E\left[\frac{\partial \mathbf{n}_x}{\partial x}\frac{\partial \mathbf{n}_z}{\partial x}\right] = 0. \quad \text{(A42)}$$

The second relation needed in the derivation of the tilt estimator is that $E[(\partial \mathbf{n}_x/\partial x)(\partial \mathbf{n}_x/\partial_y)] = 0$. The expression for $\partial \mathbf{n}_x/\partial y$ is obtained by replacing $\mathbf{P}_x$ with $\mathbf{P}_y$ and $\mathbf{Q}_x$ with $\mathbf{Q}_y$ in the expression for $\partial \mathbf{n}_x/\partial x$ [Eq. (A38)]. Expanding the expectation, we get

$$E\left[\frac{\partial \mathbf{n}_x}{\partial x}\frac{\partial \mathbf{n}_x}{\partial y}\right] = E[\{-\mathbf{n}_z + (\mathbf{n}_z-\mathbf{n}_z{}^3)\cos^2\mathbf{T}\}^2]E[\mathbf{P}_x\mathbf{P}_y]$$
$$+ E[\{(\mathbf{n}_z-\mathbf{n}_z{}^3)\sin\mathbf{T}\cos\mathbf{T}\}^2]E[\mathbf{Q}_x\mathbf{Q}_y]$$
$$+ E[-(\mathbf{n}_z{}^2-\mathbf{n}_z{}^4)]E[\sin\mathbf{T}\cos\mathbf{T}]E[\mathbf{P}_x\mathbf{Q}_y]$$
$$+ E[(\mathbf{n}_z-\mathbf{n}_z{}^3)^2]E[\sin\mathbf{T}\cos^3\mathbf{T}]E[\mathbf{P}_x\mathbf{Q}_y]$$
$$+ E[-(\mathbf{n}_z{}^2-\mathbf{n}_z{}^4)]E[\sin\mathbf{T}\cos\mathbf{T}]E[\mathbf{Q}_x{}^2]$$
$$+ E[(\mathbf{n}_z-\mathbf{n}_z{}^3)^3]E[\sin\mathbf{T}\cos^2\mathbf{T}]E[\mathbf{Q}_x{}^2]. \quad \text{(A43)}$$

The first two terms in the expression go to zero because $E[\mathbf{P}_x\mathbf{P}_y] = 0$ and $E[\mathbf{Q}_x\mathbf{Q}_y] = 0$, and the last four terms go to zero because $E[\sin\mathbf{T}\cos^n\mathbf{T}] = 0$ for all $n \geq 0$. We get

$$E\left[\frac{\partial \mathbf{n}_x}{\partial x}\frac{\partial \mathbf{n}_x}{\partial y}\right] = 0. \quad \text{(A44)}$$

The remaining relations stated in the proposition may be proved by using similar expansions.
Q.E.D.

APPENDIX B

The illuminant slant estimator presented in Section 6 of this paper makes use of the variances of the partial derivatives of image luminance that are computed in different directions in the image. The variances are functions of the variances of the partial derivatives of the components of the normal vector process $\tilde{\mathbf{N}}$. In particular, we require expressions for $E[(\partial \mathbf{n}_x/\partial x)^2]$, $E[(\partial \mathbf{n}_x/\partial y)^2]$, $E[(\partial \mathbf{n}_z/\partial x)^2]$, and $E[(\partial \mathbf{n}_z/\partial y)^2]$. Expressions for the necessary partial derivatives are derived in the proof of Proposition A6 and given in Eqs. (A39) and (A40). For $E[(\partial \mathbf{n}_x/\partial x)^2]$, we obtain

$$E\left[\left(\frac{\partial \mathbf{n}_x}{\partial x}\right)^2\right] = E[\{-\mathbf{n}_z + (\mathbf{n}_z-\mathbf{n}_z{}^3)\cos^2\mathbf{T}\}^2]E[\mathbf{P}_x{}^2]$$
$$+ E[\{(\mathbf{n}_z-\mathbf{n}_z{}^3)\sin\mathbf{T}\cos\mathbf{T}\}^2]E[\mathbf{Q}_x{}^2]$$
$$= \{E[\mathbf{n}_z{}^2] - 2E[\mathbf{n}_z{}^2]E[\cos^2\mathbf{T}]$$
$$+ 2E[\mathbf{n}_z{}^4]E[\cos^2\mathbf{T}] + E[\mathbf{n}_z{}^2]E[\cos^4\mathbf{T}]$$
$$- 2E[\mathbf{n}_z{}^4]E[\cos^4\mathbf{T}] + E[\mathbf{n}_z{}^6]E[\cos^4\mathbf{T}]\}E[\mathbf{P}_x{}^2]$$
$$+ \{E[\mathbf{n}_z{}^2]E[\sin^2\mathbf{T}\cos^2\mathbf{T}] - 2E[\mathbf{n}_z{}^4]$$
$$\times E[\sin^2\mathbf{T}\cos^2\mathbf{T}]$$
$$+ E[\mathbf{n}_z{}^6]E[\sin^2\mathbf{T}\cos^2\mathbf{T}]\}E[\mathbf{Q}_x{}^2]. \quad \text{(B1)}$$

The cross term $E[\mathbf{P}_x\mathbf{Q}_x]$ goes to zero. For the terms that contain $\mathbf{T}$, we have

$$E[\cos^2\mathbf{T}] = \frac{1}{2}, \quad \text{(B2)}$$

$$E[\cos^4\mathbf{T}] = \frac{3}{8}, \quad \text{(B3)}$$

$$E[\sin^2\mathbf{T}\cos^2\mathbf{T}] = \frac{1}{8}. \quad \text{(B4)}$$

Substituting back into Eq. (B1) and simplifying, we get

$$E\left[\left(\frac{\partial \mathbf{n}_x}{\partial x}\right)^2\right] = \left\{\frac{3}{8}E[\mathbf{n}_z{}^2] + \frac{1}{4}E[\mathbf{n}_z{}^4] + \frac{3}{8}E[\mathbf{n}_z{}^6]\right\}E[\mathbf{P}_x{}^2]$$
$$+ \left\{\frac{1}{8}E[\mathbf{n}_z{}^2] - \frac{1}{4}E[\mathbf{n}_z{}^4] + \frac{1}{8}E[\mathbf{n}_z{}^6]\right\}E[\mathbf{Q}_x{}^2]. \quad \text{(B5)}$$

To derive a term for $E[(\partial \mathbf{n}_x/\partial y)^2]$, we need merely replace $\mathbf{P}_x$ in the preceding equation with $\mathbf{P}_y$, and $\mathbf{Q}_x$ with $\mathbf{Q}_y$, giving

$$E\left[\left(\frac{\partial \mathbf{n}_x}{\partial y}\right)^2\right] = \left\{\frac{3}{8}E[\mathbf{n}_z{}^2] + \frac{1}{4}E[\mathbf{n}_z{}^4] + \frac{3}{8}E[\mathbf{n}_z{}^6]\right\}E[\mathbf{P}_y{}^2]$$
$$+ \left\{\frac{1}{8}E[\mathbf{n}_z{}^2] - \frac{1}{4}E[\mathbf{n}_z{}^4] + \frac{1}{8}E[\mathbf{n}_z{}^6]\right\}E[\mathbf{Q}_y{}^2]. \quad \text{(B6)}$$

From Proposition B3, we know that we can replace $E[\mathbf{P}_x{}^2]$ with $3E[\mathbf{P}_y{}^2]$, $E[\mathbf{Q}_x{}^2]$ with $E[\mathbf{P}_y{}^2]$, and $E[\mathbf{Q}_y{}^2]$ with $3E[\mathbf{P}_y{}^2]$, so that we can further simplify Eqs. (B5) and (B6) to

$$E\left[\left(\frac{\partial \mathbf{n}_x}{\partial x}\right)^2\right] = \left\{\frac{5}{4}E[\mathbf{n}_z{}^2] + \frac{1}{2}E[\mathbf{n}_z{}^4] + \frac{5}{4}E[\mathbf{n}_z{}^6]\right\}E[\mathbf{P}_y{}^2], \tag{B7}$$

$$E\left[\left(\frac{\partial \mathbf{n}_x}{\partial y}\right)^2\right] = \left\{\frac{3}{4}E[\mathbf{n}_z{}^2] - \frac{1}{2}E[\mathbf{n}_z{}^4] + \frac{3}{4}E[\mathbf{n}_z{}^6]\right\}E[\mathbf{P}_y{}^2]. \tag{B8}$$

These are the expressions given in Section 6 of this paper. One can also see that $E[(\partial \mathbf{n}_x/\partial x)^2] > E[(\partial \mathbf{n}_x/\partial y)^2]$ for all nonplanar isotropic surfaces, which is a fact used in the derivation of the tilt estimator.

Using Eq. (A39) to expand $E[(\partial \mathbf{n}_z/\partial x)^2]$, we obtain

$$\begin{aligned} E\left[\left(\frac{\partial \mathbf{n}_z}{\partial x}\right)^2\right] &= E[\mathbf{n}_z{}^4(1-\mathbf{n}_z{}^2)\cos^2 T]E[\mathbf{P}_x{}^2] \\ &\quad + E[\mathbf{n}_z{}^4(1-\mathbf{n}_z{}^2)\sin^2 T]E[\mathbf{Q}_x{}^2] \\ &= \{[E(\mathbf{n}_z{}^4) - E(\mathbf{n}_z{}^6)]E[\cos^2 T]\}E[\mathbf{P}_x{}^2] \\ &\quad + \{(E[\mathbf{n}_z{}^4] - E[\mathbf{n}_z{}^6])E[\sin^2 T]\}E[\mathbf{Q}_x{}^2]. \end{aligned} \tag{B9}$$

The cross term $E[\mathbf{P}_x\mathbf{Q}_x]$ goes to zero. Substituting Eqs. (B2)–(B4) for the terms that contain $\mathbf{T}$ and simplifying, we get

$$\begin{aligned} E\left[\left(\frac{\partial \mathbf{n}_z}{\partial x}\right)^2\right] &= \left\{\frac{1}{2}E[\mathbf{n}_z{}^4] - \frac{1}{2}E[\mathbf{n}_z{}^6]\right\}E[\mathbf{P}_x{}^2] \\ &\quad + \left\{\frac{1}{2}E[\mathbf{n}_z{}^4] - \frac{1}{2}E[\mathbf{n}_z{}^6]\right\}E[\mathbf{Q}_x{}^2]. \end{aligned} \tag{B10}$$

Using the relations $E[\mathbf{P}_x{}^2] = 3E[\mathbf{P}_y{}^2]$ and $E[\mathbf{Q}_x{}^2] = E[\mathbf{P}_y{}^2]$ and noting that $E[(\partial \mathbf{n}_z/\partial x)^2] = E[(\partial \mathbf{n}_z/\partial y)^2]$ for an isotropic process $\mathbf{S}$, we obtain the final result

$$E\left[\left(\frac{\partial \mathbf{n}_z}{\partial x}\right)^2\right] = E\left[\left(\frac{\partial \mathbf{n}_z}{\partial y}\right)^2\right] = \{2E[\mathbf{n}_z{}^4] - 2E[\mathbf{n}_z{}^6]\}E[\mathbf{P}_y{}^2]. \tag{B11}$$

Equations (B7), (B8), and (B11) are all that is needed for the illuminant slant estimator developed in this paper.

APPENDIX C

Implementation of the illuminant slant estimator requires a specification of the form of the local distribution of the partial derivatives of surface depth. From this specification, we can derive expressions for the moments of $\mathbf{n}_z$ that are used in the estimator. If we assume that the partial derivatives have a Gaussian distribution, which is given as

$$f_{\mathbf{P}}(p) = \frac{1}{\sqrt{2\pi}\sigma_p}\exp[-p^2/(2\sigma_p{}^2)], \tag{C1}$$

$$f_{\mathbf{Q}}(q) = \frac{1}{\sqrt{2\pi}\sigma_p}\exp[-q^2/(2\sigma_p{}^2)], \tag{C2}$$

then $\mathbf{n}_z$ will have the following distribution, as derived in Section 5:

$$f_{\mathbf{n}_z}(n_z) = \frac{\exp[1/(2\sigma_p{}^2)]}{\sigma_p{}^2 n_z{}^3}\exp[-1/(2n_z{}^2\sigma_p{}^2)], \qquad 0 < n_z \le 1. \tag{C3}$$

(Note that $\mathbf{P}$ and $\mathbf{Q}$ have the same variance $\sigma_p{}^2$, since $\mathbf{S}$ is assumed to be isotropic). The calculation of expressions for the moments of $\mathbf{n}_z$ is straightforward. For the mean of $\mathbf{n}_z$, we have

$$\begin{aligned} E[\mathbf{n}_z] &= \int_0^1 n_z f_{\mathbf{n}_z}(n_z)\mathrm{d}n_z \\ &= \int_0^1 \frac{\exp[1/(2\sigma_p)]}{\sigma_p{}^2 n_z{}^2}\exp[-1/(2n_z{}^2\sigma_p{}^2)]\mathrm{d}n_z \\ &= \frac{\sqrt{2\pi}}{\sigma_p}\exp(1/2\sigma_p{}^2)\left[1 - \mathrm{erf}\left(\frac{1}{\sqrt{2}\sigma_p}\right)\right], \end{aligned} \tag{C4}$$

where erf( ) is the standard error function. For the variance of $\mathbf{n}_z$, we have

$$\begin{aligned} E[\mathbf{n}_z{}^2] &= \int_0^1 n_z{}^2 f_{\mathbf{n}_z}(n_z)\mathrm{d}n_z \\ &= \int_0^1 \frac{\exp[1/(2\sigma_p)]}{\sigma_p{}^2 n_z}\exp[-1/(2n_z{}^2\sigma_p{}^2)]\mathrm{d}n_z \\ &= \frac{\exp[1/(2\sigma_p{}^2)]}{2\sigma_p{}^2}E_1\left(\frac{1}{2\sigma_p{}^2}\right), \end{aligned} \tag{C5}$$

where $E_n(t)$ is the nth-order exponential integral, which is defined as

$$E_n(t) = \int_t^\infty x^{-n}e^{-x}\mathrm{d}x. \tag{C6}$$

For higher-order even moments of $\mathbf{n}_z$, $E[\mathbf{n}_z{}^{2n}]$, we have

$$\begin{aligned} E[\mathbf{n}_z{}^{2n}] &= \int_0^1 n_z{}^{2n} f_{\mathbf{n}_z}(n_z)\mathrm{d}n_z \\ &= \int_0^1 \frac{\exp[1/(2\sigma_p)]}{\sigma_p{}^2}n_z{}^{2n-3}\exp[-1/(2n_z{}^2\sigma_p{}^2)]\mathrm{d}n_z \\ &= \frac{\exp[1/(2\sigma_p{}^2)]}{2^n\sigma_p{}^{2n}}E_n\left(\frac{1}{2\sigma_p{}^2}\right). \end{aligned} \tag{C7}$$

The nth-order exponential integrals are recursively related to each other by the relation

$$E_{n-1}(t) = \frac{1}{t^{n-1}}e^{-t} - (n-1)E_n(t). \tag{C8}$$

We can, therefore, derive a recursive expression for the even order moments of $\mathbf{n}_z$. This expression is given below:

$$E[\mathbf{n}_z{}^{2n}] = \frac{1}{(2n-2)\sigma_p{}^2}\{1 - E[\mathbf{n}_z{}^{2n-2}]\}, \qquad n > 1. \tag{C9}$$

For the fourth and sixth moments of $\mathbf{n}_z$, we have

$$E[\mathbf{n}_z{}^4] = \frac{1}{2\sigma_p{}^2}\{1 - E[\mathbf{n}_z{}^2]\}, \tag{C10}$$

$$E[\mathbf{n}_z{}^6] = \frac{1}{4\sigma_p{}^2}\{1 - E[\mathbf{n}_z{}^4)]\}. \tag{C11}$$

ACKNOWLEDGMENTS

This research was supported by National Science Foundation grant BNS-8708532 to Daniel Kersten and by National Science Foundation grant BNS-85-18675 to James Anderson. The author thanks Dan Kersten and James Anderson for their unwavering support and helpful comments.

REFERENCES AND NOTES

1. K. Ikeuchi and B. K. P. Horn, "Numerical shape from shading and occluding boundaries," Artif. Intell. **17,** 141–184 (1981).
2. C. H. Lee and A. Rosenfeld, "Improved methods of estimating shape from shading using the light source coordinate system," Artif. Intell. **26,** 125–143 (1985).
3. D. C. Knill and D. Kersten, "Learning a near optimal estimator for surface shape from shading," Comput. Vision Graphics Image Process. (to be published).
4. A. P. Pentland, "The visual inference of shape: computation from local features," Ph.D. dissertation (Massachusetts Institute of Technology, Cambridge, Mass., 1982).
5. A. P. Pentland, "Finding the illuminant direction," J. Opt. Soc. Am. **72,** 448–455 (1982).
6. This is a weaker condition than sample differentiability, which would require that all samples of the process were differentiable.
7. The variance of a random variable $\mathbf{X}$ is defined as $\mathrm{Var}[\mathbf{X}] = E[\mathbf{X}^2] - E[\mathbf{X}]^2$. For most cases presented in this paper, $E[\mathbf{X}] = 0$, and the variance reduces to $\mathrm{Var}[\mathbf{X}] = E[\mathbf{X}^2]$. To be more compact, we use $E[\mathbf{X}^2]$ to refer to variance when the mean of the random variable (or stochastic process) in question is zero.
8. Staff of the Research and Education Association, *Handbook of Mathematical, Scientific, and Engineering Formulas, Tables, Functions, Graphs, Transforms* (Research and Education Association, New York, 1984).
9. H. J. Larson and B. O. Shubert, *Random Noise, Signals and Dynamic Systems* Vol. 2 of Probabilistic Models in Engineering Science (Wiley, New York, 1979).